

A novel nature-inspired nutcracker optimizer algorithm for congestion control in power system transmission lines

Energy Exploration & Exploitation
1–36

© The Author(s) 2024
DOI: 10.1177/01445987241253292
journals.sagepub.com/home/eea



Vivek Kumar¹, R Narendra Rao², Ajendra Singh³,
Vineet Shekher⁴, Kaushik Paul⁴ , Pampa Sinha⁵,
Thamer AH Alghamdi^{6,7} and Almoataz Y Abdelaziz⁸

Abstract

In the restructured power system, where uncertainties are common, managing congestion becomes a crucial aspect of power system operation and control. Congestion management aims to alleviate the power system transmission line congestion while meeting the system constraints at minimal cost. This research introduces a generation rescheduling method for congestion management in the electricity market, leveraging an innovative nutcracker optimizer algorithm. The nutcracker optimizer algorithm, inspired by nutcrackers' food accumulation mechanisms, is a recently developed nature-inspired algorithm. The efficacy of this proposed approach is assessed across modified IEEE 30-bus, and IEEE 118-bus test systems, considering the system parameters. The effectiveness of the proposed congestion management with the nutcracker optimizer algorithm is analyzed by comparing its results with those generated by other recent optimization techniques. Results demonstrated that the nutcracker optimizer algorithm surpasses other comparative methods, requiring fewer fitness function evaluations, avoiding local optima, and displaying encouraging convergence traits. Implementing this approach can assist the system

¹Department of Electrical Engineering, BRCM College of Engineering & Technology, Bhiwani, Haryana, India

²Department of Electrical and Electronics Engineering, JNTUA College of Engineering Pulivendula, Pulivendula, India

³Department of Electrical Engineering, Delhi Technological University, Delhi, India

⁴Department of Electrical Engineering, BIT Sindri, Dhanbad, India

⁵School of Electrical Engineering, KIIT University, Bhubaneswar, Orissa, India

⁶Electrical Engineering Department, College of Engineering, Al-Baha University, Al-Baha, Saudi Arabia

⁷Wolfson Centre for Magnetics, School of Engineering, Cardiff University, Cardiff, UK

⁸Faculty of Engineering and Technology, Future University in Egypt, Cairo, Egypt

Corresponding author:

Kaushik Paul, Department of Electrical Engineering, BIT Sindri, Dhanbad 828123, India.

Email: kaushik.ee@bitsindri.ac.in

Thamer AH Alghamdi, Wolfson Centre for Magnetics, School of Engineering, Cardiff University, Cardiff, CF24 3AA, UK.

Email: Alghamdi1@cardiff.ac.uk



operators in swiftly addressing contingencies, ensuring secure and reliable power system operation within a deregulated environment.

Keywords

Energy, power flow, evolutionary algorithm, power system, optimization, rescheduling

Introduction

The ability of transmission lines to carry electrical power is limited by various factors, including voltage, heat, and stability. When any of these limits is reached, the power system is considered congested. Congestion can have significant implications on the power dispatch, potentially impacting the overall performance of the system. Managing power system congestion is a critical task undertaken by independent system operators (ISOs) and grid operators (Bouhouras et al., 2024). They play a crucial role in coordinating and overseeing the functioning of the power market, ensuring efficient power flow, and maintaining system stability. With the increasing demand for electricity, aging infrastructure, and limitations on new transmission line construction, congestion has become a prevalent issue in power systems worldwide (Alavijeh et al., 2024).

Several factors contribute to congestion. These include an upsurge in power demand beyond the infrastructure's capacity, unexpected generation outages, limitations on building new transmission lines due to environmental or logistical constraints, unscheduled power flow, transmission line tripping, or equipment failures. The resulting congestion can lead to reduced reliability, increased energy costs, and potential disruptions in power supply to consumers (Dehnavi et al., 2024). To address congestion effectively, various congestion management (CM) strategies are employed. These strategies aim to alleviate constraints, optimize power flow, and maintain system stability. Some common approaches include reactive power support, generation rescheduling, demand response programs, transmission line reconfiguration, and dispatching of power resources (Ansari et al., 2020; Shaikh et al., 2020; Zhou et al., 2023). These methods help balance the power system and mitigate congestion-related issues, ensuring reliable and uninterrupted electricity supply to consumers.

Literature survey

In recent years, advancements in technology, such as smart grid technologies, advanced metering infrastructure, and real-time monitoring systems, have provided enhanced capabilities for CM. These tools enable grid operators to gather precise data, monitor system conditions, and implement timely control actions to alleviate congestion and optimize power flow. Zaidan and Toos proposed an emergency CM method for power systems using a static synchronous series compensator (SSSC). The authors focused on alleviating congestion during emergency situations and introduced the SSSC as a device to enhance the power transfer capability of transmission lines (Majeed Rashid Zaidan, 2022). The research focuses on optimizing transmission line parameters using an enhanced moth flame optimization technique, demonstrating its superiority over other methods through simulations on various test cases. Results indicate that the proposed method achieves rapid convergence to optimal values for capacitance and inductance, showcasing its effectiveness and competence in managing transmission and distribution networks (Shaikh et al., 2022c). Wang et al. introduced the concept of virtual storage plants (VSPs) for frequency regulation and CM in power systems. They proposed a framework where distributed energy resources are aggregated into VSPs to provide

ancillary services for frequency regulation and CM. The study evaluates the performance of the VSP and its potential for improving the stability and efficiency of power systems (Wang et al., 2022). Managing the transmission line flows with the influence of optimization algorithm for transmission line parameter optimization can be found in (Shaikh et al., 2021a, 2022a, 2022b, 2023). Mahajan et al. provided a review of CM in deregulated power systems. The review associated with the CM summarized the existing literature on CM techniques, including market-based approaches, generation rescheduling, load shedding, and demand response programs. The review also provided insights into the challenges and opportunities in managing congestion in deregulated power systems (Mahajan et al., 2022). Hobbie et al. investigated the effect of model parametrization of the transmission channels during the congested environment of the power system. The authors compare different existing models used for CM in electricity networks and analyze the influence of model parameters on CM (Hobbie et al., 2022). Zakaryaseraji and Ghasemi-Marzbali evaluated CM in power systems considering demand response programs and distributed generation (DG). They incorporated demand response and DG as flexible resources for managing congestion (Zakaryaseraji and Ghasemi-Marzbali, 2022). Shaikh et al. conducted their research to select the optimal transmission-line parameters that would assist efficient power flows (Shaikh et al., 2021b). Roustaei et al. formulated a voltage security-constrained CM methodology for improving the controlling of transmission systems. They addressed the challenges of voltage security and CM and proposed an approach that optimizes generation rescheduling to alleviate congestion while considering voltage security constraints (Roustaei et al., 2022). In another research, Mishra et al. provided a review of the utilization of AI-based methods in alleviating the congestion of transmission channels considering the electricity market constraints. The review mainly highlighted the application of artificial intelligence techniques, such as neural networks, fuzzy logic, and evolutionary algorithms, for CM in restructured power systems (Mishra et al., 2022). Paul formulated an enhanced framework of a grey wolf optimization algorithm that controls the congestion considering the impact of renewable sources. The CM focused on optimizing the operation of transmission lines to alleviate congestion and incorporates the impact of solar photovoltaic systems in the optimization process (Paul, 2022a). Dehnavi et al. proposed a novel CM method through power system partitioning. In the CM approach, they considered the power system into multiple partitions and applied a decentralized control strategy to manage congestion (Dehnavi et al., 2022). Sarwar et al. developed an effective transmission CM approach for contemporary power system operations using optimal DG capacity and hybrid swarm optimization. The authors focused on determining the optimal capacity of DG units at specific locations in the power system to mitigate congestion (Sarwar et al., 2022).

In the CM, generator rescheduling (GR) plays a crucial role by optimizing the generation dispatch to alleviate congestion. It allows for the efficient utilization of existing transmission infrastructure, reducing the need for costly grid expansion. By strategically adjusting generator schedules, congestion can be alleviated, ensuring reliable and secure power system operation. GR also enables the integration of renewable energy sources and promotes the economic dispatch of generation resources, leading to enhanced system efficiency and cost-effectiveness. Subramaniyan and Gomathi presented a soft computing-based analysis of CM in transmission systems with the application of generator rescheduling. The CM approach explored the application of soft computing techniques, such as fuzzy logic and genetic algorithms, for managing congestion (Subramaniyan and Gomathi, 2023). Agrawal et al. proposed a cascaded deep neural network-based approach for customer participation in CM, considering renewable energy sources and GR in deregulated power markets. Their research focused on optimizing the participation of customers with distributed energy resources to alleviate congestion (Agrawal et al., 2022). Chakravarthi et al. investigated real-time CM using generation redispatch. They designed controllers for efficient

generation rescheduling to mitigate congestion in power systems (Chakravarthi et al., 2022). Srivastava and Yadav proposed a rescheduling-based CM approach using a hybrid algorithm that combines lion and moth search models. The authors optimized generator schedules to alleviate congestion and enhance the operational efficiency of power systems (Srivastava and Yadav, 2021). Ogunwole and Krishnamurthy developed a transmission CM approach using generator sensitivity factors and particle swarm optimization. The authors focus on optimizing active and reactive power rescheduling to alleviate congestion and enhance system performance (Ogunwole and Krishnamurthy, 2022). Prajapati et al. proposed a GR-based CM approach considering the demand response characteristic for power systems and uncertainty of the renewable resources (Thiruvel et al., 2023) and presented a modern power system operations approach for effective transmission CM using optimal distributed generation (DG) capacity and GR. The authors determined the optimal capacity of DG units and real power deliveries by the generators to alleviate congestion (Thiruvel et al., 2023). Balaraman and Kamaraj managed congestion for a deregulated electricity market with the application of GR methodology. They implemented particle swarm optimization (PSO) to alleviate overloads and minimize deviations from the initial market settlement. The PSO application for CM addressed system constraints security constraints, using a penalty-based approach (Kamaraj, 2011). Saravanan and Anbalagan proposed an intelligent hybrid technique for optimal GR in deregulated power markets. They combined genetic algorithms (GA) and PSO to optimize generator schedules and alleviate congestion (Saravanan and Anbalagan, 2022). Sharma and Walde proposed a novel optimization technique based on swarm intelligence for CM in transmission lines. They applied a hybrid algorithm combining PSO and GSA to optimize power flow and alleviate congestion (Sharma and Walde, 2022). Haq et al. proposed a game-theoretic approach using plug-in electric vehicles (PEVs) and GR for real-time CM. Their work investigated the participation of PEVs and GR in alleviating congestion by adjusting their charging and discharging patterns (Haq et al., 2022). Verma and Mukherjee implemented real power GR rescheduling using a novel ant lion optimizer for CM. The CM approach aimed at optimizing generator schedules to alleviate congestion and enhance power system performance (Verma and Mukherjee, 2016b). Paul et al. reduced rescheduling costs and efficiently alleviated line overloads with minimal deviations in active power generation. The developed CM strategy involved prioritizing generators based on their sensitivity values. The GSA is then employed to minimize rescheduling costs while simultaneously reducing total active power output and system losses (Paul et al., 2019).

The emergence of competitive energy markets has driven the advancement of optimization algorithms that effectively tackle mathematical problems related to power system challenges, resulting in precise and improved outcomes. The classical optimization methods have been widely used and effective in certain scenarios but have some limitations that make metaheuristic optimization methods more preferable in many cases. Classical optimization methods have limitations such as getting entombed in local optima, sensitivity to initial conditions, lack of flexibility, high computational cost, and difficulty in handling uncertainties and noisy environments. In contrast, metaheuristic algorithms overcome these limitations by exploring the entire solution space, being less sensitive to initial conditions, offering flexibility in problem domains, providing computational efficiency, and accommodating uncertainties and noisy environments through robust and adaptive mechanisms. The metaheuristic algorithms strike a balance between exploration (diversification) and exploitation (intensification) of the search space. They avoid getting stuck in local optima by exploring different regions while also exploiting promising areas. This ability to balance exploration and exploitation enhances their capability to find better solutions. Various approaches such as grey wolf optimization (Paul, 2022b), Fennec Fox optimization (Verma and Mukherjee, 2016a), flower pollination algorithm (FPA; Gupta et al., 2023), cuckoo search algorithm (CSA; Wangunyu et al., 2022), and an enhanced version of crow search algorithm (CSA) (Paul et al., 2022) have been implemented to oversee the efficient operation of power

systems. The selection and adjustment of control parameters associated with these meta-heuristic techniques greatly influence the achieved solution. This has motivated the development of an efficient CM strategy with the application of the evolutionary algorithm that will deliver optimal outcomes for the optimization problem.

The novelty can be stated as the minimization of the congestion cost/rescheduling cost always creates a scope for implementation of new efficient optimization approaches that would deliver appreciable outcomes w.r.t previously adopted approaches. The integral novelty of this paper lies in the mathematical model formulation of the congestion cost minimization with the incorporation of the new nutcracker optimization algorithm (NOA).

In this research work, NOA which is a new metaheuristic optimization technique has been considered for the CM problem. The NOA has been designed by Basset et al. in the year 2023 (Abdel-Basset et al., 2023). The framework of NOA is inspired by the intelligent behaviors of nutcrackers to search for and store food. It draws inspiration from the hunting behavior of antlions. According to Abdel-Basset et al. (2023), the NOA has been validated on standard mathematical functions (CEC-2014, CEC-2017, and CEC-2020) and classical engineering problems. The findings presented by Abdel-Basset et al. (2023) demonstrated the advantages of the NOA in terms of improved exploration capabilities.

Motivation

The primary motivation behind this endeavor is to devise a proficient approach for CM aimed at enhancing the efficiency of power system operations. The competitive dynamics and trading behavior within the electricity market have heightened the vulnerability of the power network to congestion, prompting researchers in the field to investigate various CM strategies for their applicability and effectiveness. Given the extensive scale of the power network, any implemented CM strategy must possess qualities of robustness, effectiveness, and cost-efficiency, and must not disrupt the network's existing topology. Thus, in light of these considerations, the implementation of the generators rescheduling (GR) approach emerges as a fitting solution for CM. Furthermore, in power system operations, it's imperative to mitigate congestion at minimal cost, necessitating the utilization of efficient optimization techniques that yield optimal cost solutions. While many optimization techniques exhibit commendable performance, they often become ensnared in local optima, unable to navigate the search space effectively to identify the optimal solution. Consequently, there's a strong impetus to enhance the performance of optimization techniques by refining their operational stages. This drive has spurred advancements in the efficiency of exploration and exploitation stages within the NOA.

Research contribution

- Development of a CM model to minimize the congestion cost based on the optimal rescheduling of the generators' real power.
- Implementation of NOA to achieve the optimal power rescheduling patterns for generators for congestion cost minimization.
- Application of the CM strategies on power stream standard test system; IEEE 30-bus and IEEE 118-bus to validate the efficiency of the proposed CM model.
- Establish comparative performance analysis based on the congestion cost, bus voltage profile, and system losses achieved with NOA with the recent optimization techniques.

Problem formulation

The primary goal of CM is to reduce the expenses caused by congestion while adhering to the limitations of the network. This study addresses the CM problem by adjusting the actual power output of generators, either increasing or decreasing it. However, modifying the real power output incurs costs that are decided based on the price offers provided by the generating companies. This can be represented as.

$$\min CC = \sum_{n=1}^{N_g} (C_{inc} \cdot \Delta P_g + C_{dec} \cdot \Delta P_g) \$ / h \quad (1)$$

The equation involves various variables: CC represents the aggregated cost of adjusting real power in $\$/h$, C_{inc} and C_{dec} denotes the incremental and decremental price bids, respectively, ΔP_g is the adjusted power by the generators. The constraints considered for this optimization problem are as follows:

Inequality constraints

These constraints are expressed through the following equations:

$$P_{Gn}^{\min} \leq P_{Gn} \leq P_{Gn}^{\max}; \quad \forall n \in N_g \quad (2)$$

$$Q_{Gn}^{\min} \leq Q_{Gn} \leq Q_{Gn}^{\max}; \quad \forall n \in N_g \quad (3)$$

$$(P_{Gn} - P_{Gn}^{\min}) = \Delta P_{Gn}^{\min} \leq \Delta P_{Gn} \leq \Delta P_{Gn}^{\max} = (P_{Gn}^{\max} - P_{Gn}); \quad \forall n \in N_g \quad (4)$$

$$V_n^{\min} \leq V_n \leq V_n^{\max} \quad (5)$$

$$P_{ij} \leq P_{ij}^{\max} \quad (6)$$

Equality constraints

$$P_{Gn} - P_{Dn} = \sum_j |V_j| |V_k| |Y_{kj}| \cos(\delta_k - \delta_j - \theta_{kj}); \quad j = 1, 2, 3, \dots, N_b \quad (7)$$

$$Q_{Gn} - Q_{Dn} = \sum_j |V_j| |V_k| |Y_{kj}| \sin(\delta_k - \delta_j - \theta_{kj}); \quad j = 1, 2, 3, \dots, N_b \quad (8)$$

$$P_{Gn} = P_{Gn}^C + \Delta P_{Gn}^+ - \Delta P_{Gn}^-; \quad k = 1, 2, 3, \dots, N_g \quad (9)$$

$$P_{Dj} = P_{Dj}^C; \quad j = 1, 2, 3, \dots, N_d \quad (10)$$

Here, in equations (7) and (8), P_{Gk} and Q_{Gk} represent the active and reactive powers generated at the k th bus, respectively. Similarly, P_{Dk} and Q_{Dk} denote the active and reactive powers at the k th bus,

respectively. In equations (7) and (8), V_j and V_k indicate the voltages at buses, while δ_k and δ_j are the bus voltage angles. The parameter θ_{kj} represents the admittance angle. The count of the generators, buses and loads are given by N_b , N_g , and N_d , respectively. P_{Gk}^C is the generated power and P_{Dj}^C is the consumed by the load. It should be noted that equations (7) and (8) outline the balances of active and reactive power at individual nodes, whereas equations (9) and (10) portray the resulting power in relation to the market clearing price.

Nutcracker optimizer algorithm

This section presents a bio-inspired optimization algorithm (NOA) that draws inspiration from the intelligent behaviors of nutcrackers. The NOA has been designed by Basset et al. in the year 2023 (Abdel-Basset et al., 2023). The nutcracker's behavior can be segregated and portrayed into two sections. The first part involves collecting and storing pine seeds as food. The second part involves searching for and retrieving the stored seeds.

Foraging stage: Exploration phase I

In the starting position, each nutcracker examines the cone holding seeds; if good seeds are found, they are taken to the storage area for burial. If no good seeds are found, the nutcracker seeks another cone among pine/trees. The mathematical representation of this behavior representing the position update can be stated as

$$\vec{Z}_i^{t+1} = \begin{cases} Z_{i,j}^t; & \text{if } \tau_1 < \tau_2 \\ Z_{m,j}^t + \psi(Z_{A,j}^t - Z_{B,j}^t) + \xi(r^2 U_j - L_j); & \text{if } t \leq T_{\max} / 2.0 \\ Z_{C,j}^t + \xi(Z_{A,j}^t - Z_{B,j}^t) + \xi(r^2 U_j - L_j); & \text{otherwise} \end{cases} \quad (11)$$

\vec{Z}_i^{t+1} denotes the current position of the i th nutcracker, and $Z_{i,j}^t$ represents its j th position. Vectors U_j and L_j define the upper and lower bounds of the j th dimension in the optimization problem, respectively. ψ is a randomly generated number using the levy flight. $\vec{Z}_{best,j}^t$ signifies the j th dimension of the best solution. τ_1 , τ_2 , and r ranges $[0, 1]$. $Z_{m,j}^t$ is the mean of all solutions. In equation (12), ξ is generated based on the normal distribution (τ_4), levy-flight τ_5 , and τ_3 $[0, 1]$.

Top of form

$$\xi = \begin{cases} \tau_3 & \text{if } r_1 < r_1 \\ \tau_4 & \text{if } r_2 < r_3 \\ \tau_5 & \text{if } r_1 < r_3 \end{cases} \quad (12)$$

In this scenario, r_1 , r_2 , and r_3 are arbitrary real numbers between 0 and 1. Equation (11) has been created to study top-notch food options. The initial part of equation (11) shows how likely it is for nutcrackers to find good seeds on their first try, suggesting they won't change the original dimension in the solution Z_i^t . Equation's (11) second stage helps nutcrackers explore the search space globally, boosting NOA's search power. In the third stage, nutcrackers explore positions near a randomly chosen solution while keeping the chance to move globally with a δ probability. A and B offer data on new food spots, while τ_1 and τ_2 regulate NOA's exploration. The algorithm switches between local and global searches using diverse τ_1 and τ_2 values. μ guides nutcrackers with directions and step sizes for exploring new positions.

Storage stage: Exploitation phase 1

Initially, nutcrackers traverse with the gathered foodstuff in the prior exploration phase, called phase 1, to interim stowing in the storage area. This phase is termed “exploitation phase 1” as it involves both exploiting and storing pine seed crops. This behavior can be mathematically represented as:

$$\vec{Z}_i^{t+1(new)} = \begin{cases} \vec{Z}_i^t + \xi \cdot (\vec{Z}_{best}^t - \vec{Z}_i^t) \cdot |\gamma| + r_1 \cdot (\vec{Z}_A^t - \vec{Z}_B^t) & \text{if } \tau_1 < \tau_2 \\ \vec{Z}_{best}^t + \xi \cdot (\vec{Z}_A^t - \vec{Z}_B^t) & \text{if } \tau_1 < \tau_3 \\ \vec{Z}_{best}^t \cdot l & \text{otherwise} \end{cases} \quad (13)$$

In the current iteration, the position of a new item in the storage area of the nutcrackers is represented by a vector $\vec{Z}_i^{t+1(new)}$. \vec{Z}_{best}^t represents the j th dimension of the best solution obtained so far. The value of γ is determined by a Lévy flight, while τ_3 is a random number between 0 and 1. The factor l gradually decreases from 1 to 0, aiding in broadening NOA’s exploitation behavior, this diversity in approach speeds up convergence and avoids getting stuck in local minimums that may occur when exploring in just one direction.

Throughout the optimization process, a consistent equilibrium between exploration and exploitation operators is upheld by applying the following formula to regulate the interaction between the foraging stage and the cache:

$$\vec{Z}_i^{t+1} = \begin{cases} \text{Equation (11), if } \phi > P_{a1} \\ \text{Equation (13), otherwise} \end{cases} \quad (14)$$

In this stage, a random number ϕ is generated between zero and one, and the probability value P_{a1} gradually decreases from one to zero. The generated solutions are directed towards a specific region to cover as many solutions as possible.

Cache-search and recovery strategy

- Cache-search stage: Exploration phase 2: Nutcrackers employ spatial memory tactics to uncover their caches, where multiple objects might signify a single cache. Each cache corresponds to just two markers or objects, known as reference points (RPs). Within the NOA, two RPs are established for each population’s cache/nutcracker using the following matrix:

$$RPs = \begin{bmatrix} RP_{1,1}^t & RP_{1,2}^t \\ \vdots & \vdots \\ RP_{i,1}^t & RP_{i,2}^t \\ \vdots & \vdots \\ RP_{n,1}^t & RP_{n,2}^t \\ \vdots & \vdots \end{bmatrix} \quad (15)$$

In this equation, $RP_{i,1}^t$ and $RP_{i,2}^t$ stand for the RPs linked to the i th nutcracker’s cache position \vec{Z}_i^t at generation t .

Nutcrackers find caches accurately, but about 20% of attempts fail initially. If they cannot locate the food with the first RP, they try the second RP. Failing that, they turn to the third reference. Two equations boost nutcrackers' exploration for caches. The first *RP* updates the position to uncover nearby caches. Its formula is

$$\overrightarrow{RP}_{i,k}^t = \overrightarrow{Z}_i^t + \alpha \cdot \cos(\theta) \cdot ((\overrightarrow{Z}_A^t - \overrightarrow{Z}_B^t)), k = 1 \quad (16)$$

The second RP adjusts the existing solution to assist nutcrackers explore diverse areas. Its calculation follows a specific formula:

$$\overrightarrow{RP}_{i,k}^t = \overrightarrow{Z}_i^t + \alpha \cdot \cos(\theta) \cdot ((\overrightarrow{U} - \overrightarrow{L}) \cdot \tau_3 + \overrightarrow{L}) \cdot \overrightarrow{U}_2; k = 2 \quad (17)$$

$$\overrightarrow{U} = \begin{cases} 1; & r_2 < P_{rp} \\ 0; & \text{otherwise} \end{cases} \quad (18)$$

Equations (16) and (17) create two RPs for each nutcracker, aiding in cache recovery. Close RPs make retrieval easier; initially, nutcrackers lack experience but learn over time. In the equations, α trains nutcrackers, preventing RPs from converging too soon. θ , randomly picked from 0 to π .

When $\theta = \pi/2$, $\overrightarrow{RP}_{i,k}^t$ matches \overrightarrow{Z}_i^t which portrays their overlap. To handle this, equations (16) and (17) can be combined and represented as

$$\overrightarrow{RP}_{i,1}^t = \begin{cases} \overrightarrow{Z}_i^t + \alpha \cdot \cos(\theta) \cdot ((\overrightarrow{Z}_A^t - \overrightarrow{Z}_B^t)) + \alpha \cdot RP; & \text{if } \theta = \pi/2 \\ \overrightarrow{Z}_i^t + \alpha \cdot \cos(\theta) \cdot ((\overrightarrow{Z}_A^t - \overrightarrow{Z}_B^t)); & \text{otherwise} \end{cases} \quad (19)$$

$$\overrightarrow{RP}_{i,2}^t = \begin{cases} \overrightarrow{Z}_i^t + (\alpha \cdot \cos(\theta) \cdot ((\overrightarrow{U} - \overrightarrow{L}) \cdot \tau_3 + \overrightarrow{L}) + \alpha \cdot RP) \cdot \overrightarrow{U}_2; & \text{if } \theta = \pi/2 \\ \overrightarrow{Z}_i^t + \alpha \cdot \cos(\theta) \cdot ((\overrightarrow{U} - \overrightarrow{L}) \cdot \tau_3 + \overrightarrow{L}) \cdot \overrightarrow{U}_2; & \text{otherwise} \end{cases} \quad (20)$$

$\overrightarrow{RP}_{i,1}^t$ refers to the element in the i th row and first column of the matrix in equation (15), while $\overrightarrow{RP}_{i,2}^t$ is in the i th row and second column of the same matrix. Each row corresponds to a cache/nutcracker, each column to an *RP*. *RP* means a random position. To avoid *RPs* converging too soon, the third term in equations (19) and (20) ($\theta = \pi/2$) is added. α ensures regular convergence in NOA, improving RP selection in later generations. Calculate α with this equation:

$$\alpha = \begin{cases} \left(1 - \frac{t}{T_{\max}}\right)^{2 \cdot \frac{t}{T_{\max}}}; & \text{if } r_1 > r_2 \\ \left(\frac{t}{T_{\max}}\right)^2; & \text{otherwise} \end{cases} \quad (21)$$

In this case, t is the current generation, and T_{\max} is the maximum number of generations. The first stage in equation (21) decreases with each round, speeding up convergence. Meanwhile, the second stage rises gradually to avoid trapping the algorithm in local lows caused by the first stage.

During optimization, nutcrackers gain expertise in *RP* selection. They adjust their storage based on these RPs. In NOA, all nutcrackers explore promising regions using an exploration mechanism. Progressively, the algorithm avoids local lows by dynamically exploring and exploiting areas

around caches with suitable RP s. The nutcracker's updated position follows this equation:

$$\vec{Z}_i^{t+1} = \begin{cases} \vec{Z}_i^t; & \text{if } f(\vec{Z}_i^t) \text{lt}(\overrightarrow{RP}_{i,1}^t) \\ \overrightarrow{RP}_{i,1}^t; & \text{otherwise} \end{cases} \quad (22)$$

The equation demonstrates the new cache \vec{Z}_i^{t+1} of the i th nutcracker in iteration $(t+1)$, where \vec{Z}_i^t represents the current cache, and $\overrightarrow{RP}_{i,1}^t$ is the initial link associated with the current cache in iteration t . Equation (22) steers NOA toward exploring and exploiting areas near $\overrightarrow{RP}_{i,1}^t$.

- *Recovery stage: Exploitation phase 2:* The main scenario: a nutcracker recalls the cache with the first RP . Figure 8 shows two options: food present or absent. Mathematically, it's expressed as follows:

$$\vec{Z}_{ij}^{t+1} = \begin{cases} \vec{Z}_{ij}^t; & \text{if } \tau_3 < \tau_4 \\ \vec{Z}_{ij}^t + r_1 \cdot (\vec{Z}_{best,j}^t - \vec{Z}_{ij}^t) + r_2(\overrightarrow{RP}_{ij}^t - \vec{Z}_{ij}^t); & \text{otherwise} \end{cases} \quad (23)$$

Let \vec{Z}_{ij}^{t+1} be the updated cache, \vec{Z}_{ij}^t is the current dimension, and $\vec{Z}_{best,j}^t$ shows the best cache found so far in iteration t . $\overrightarrow{RP}_{ij}^t$ is the random parameter of the i th nutcracker's current cache in iteration t . r_1, r_2, τ_3 , and τ_4 ranges between $[0, 1]$.

Equation's (23) first condition assumes food is present, passing certain dimensions to the consecutive generation. The second condition in equation (23) assumes no food, signaling an unpromising solution; an escape mechanism avoids local lows. Food loss in the cache could be due to theft or natural elements. The first part of equation (23) helps the nutcracker exploit promising areas locally. The second part allows exploration globally in the search space.

If the nutcracker cannot find food with the first RP , it tries the second one. Nutcrackers store multiple RP s in early storage, but sometimes the first RP fails. Some rely on changing landmarks when autumn becomes winter. Equation (24) updates nutcracker memory with the second RP .

$$\vec{Z}_i^{t+1} = \begin{cases} \vec{Z}_i^t; & \text{if } f(\vec{Z}_i^t) \text{lt}(\overrightarrow{RP}_{i,2}^t) \\ \overrightarrow{RP}_{i,2}^t; & \text{otherwise} \end{cases} \quad (24)$$

In this setting, \vec{Z}_i^t is the current cache, and $\overrightarrow{RP}_{i,2}^t$ is the second RP linked to the i th nutcracker. Equation (24) enables NOA to observe new locations within the vicinity of the second RP and perform exploitation within the most prominent areas. In NOA, finding the cache with the second RP updates equation (13) based on this information.

$$\vec{Z}_{ij}^{t+1} = \begin{cases} \vec{Z}_{ij}^t; & \text{if } \tau_5 < \tau_6 \\ \vec{Z}_{ij}^t + r_1 \cdot (\vec{Z}_{best,j}^t - \vec{Z}_{ij}^t) + r_2(\overrightarrow{RP}_{i,2}^t - \vec{Z}_{ij}^t); & \text{otherwise} \end{cases} \quad (25)$$

In the given equation, r_1, r_2, τ_5 , and τ_6 are random numbers from 0 to 1. Equation's (25) first part intensifies local search in optimal areas. The second part explores new spaces for a better global

search.

$$\vec{Z}_i^{t+1} = \begin{cases} \text{Equation (13), if } \tau_7 < \tau_8 \\ \text{Equation (15), otherwise} \end{cases} \quad (26)$$

In this equation, τ_7 and τ_8 are random numbers from 0 to 1. First case: nutcracker recalls the store; second: cannot remember. Equation balances exploration between the two RPs:

$$\vec{Z}_i^{t+1} = \begin{cases} \text{Equation (12), if } f(\text{equation (12)}) < f(\text{equation (14)}) \\ \text{Equation (14), otherwise} \end{cases} \quad (27)$$

To sustain a steadiness between exploration and exploitation, the transition between the cache-search phase and the recovery phase is executed through the utilization of the subsequent formula.

$$\vec{Z}_i^{t+1} = \begin{cases} \text{Equation (16), if } \phi < P_{a2} \\ \text{Equation (17), otherwise} \end{cases} \quad (28)$$

In this equation, ϕ ranges from 0 to 1, and P_{a2} is set at 0.2 based on several trial runs, and the best result is obtained from stand benchmark functions.

Performance analysis of NOA

The NOA's performance has been evaluated across 23 standard benchmark functions, including seven unimodal and 13 multimodal functions. The details of these functions can be found by Dolatabadi et al. (2020). Comparisons with GTO, AHA, and the original NOA are conducted. In this study, search agents and maximum iterations are set at 40 and 500, respectively, with findings gathered from 30 separate runs. Results show that NOA exhibits significant performance during both the exploration and exploitation stages. Table 1 provides the average (Avg), standard deviation (SD), median (Med), and worst (worst of the best-so-far solution) values obtained for GTO, AHA, and NOA the original MRFO in the final repetition. The test results with 23 benchmark functions are given in Table 1. Convergence profiles of the 23 benchmark functions using NOA, AHA, and GTO are depicted in Figure 1, while Figure 2 illustrates the flowchart for NOA in addressing the proposed CM problem.

Computational complexity of NOA

The evaluation of algorithm complexity in dimensions 20, 40, and 50 is conducted according to the guidelines outlined by Liang et al. (2013) and the results are illustrated in Table 2. The runtime is determined through the assessment of the CEC 2014 benchmark function FCEC18. The determination of T_0 is accomplished resulting in a computed execution time of $T_0 = 0.7539$ s. T_1 signifies the duration required for executing 2.00×10^5 evaluations of the benchmark function FCEC18 individually across dimensions of 20, 40, and 50. Meanwhile, T_2 denotes the time taken for executing an algorithm encompassing 2.00×10^5 evaluations of FCEC18 in 20, 40, and 50 dimensions.

Results

The proposed NOA is tested on three different power systems: the modified IEEE 30-bus (Sharma et al., 2018) and IEEE 118-bus test systems (Dash and Mohanty, 2015). The necessary data for these systems is obtained from Paul (2022b) and Paul et al. (2022). In addition to applying the

Table I. Performance of NOA, GTO, and AHA on 23 benchmark functions.

Functions		NOA	GTO	AHA
F1	Avg	0	1.82×10^{-43}	2.77×10^{-27}
	SD	0	1.9×10^{-43}	8.68×10^{-27}
	Med	0	1.56×10^{-43}	2.27×10^{-29}
	Worst	0	7.9×10^{-43}	4.59×10^{-26}
F2	Avg	0	7.61×10^{-26}	1.27×10^{-19}
	SD	0	7.12×10^{-26}	3.05×10^{-20}
	Med	0	6.19×10^{-26}	7.67×10^{-23}
	Worst	0	2.72×10^{-25}	7.94×10^{-20}
F3	Avg	0	0.186	4.58×10^{-8}
	SD	0	0.133	0.000000128
	Med	0	0.131	3.95×10^{-12}
	Worst	0	0.131	0.000000407
F4	Avg	0	0.000000211	2.54×10^{-9}
	SD	0	8.88×10^{-8}	5.46×10^{-9}
	Med	0	0.00000019	4.81×10^{-11}
	Worst	0	0.000000339	0.000000168
F5	Avg	931.2192	3.2	7.118
	SD	2396.3352	2.2	0.25018
	Med	135.1696	2.78	7.2289
	Worst	7710.4457	6.68	7.3661
F6	Avg	0	0	0.31179
	SD	0	0	0.11916
	Med	0	0	0.29383
	Worst	0	0	0.48389
F7	Avg	0.0000157	0.0028	0.0007298
	SD	0.0000141	0.00103	0.0005702
	Med	0.000012	0.0026	0.0006444
	Worst	0.0000531	0.00478	0.0020895
F8	Avg	-2665.515	-4170	-2313.3951
	SD	223.8271	50	248.3506
	Med	-2634.759	-4190	-2197.3255
	Worst	-2400.079	-4070	-2136.702
F9	Avg	0	0	1.5968
	SD	0	0	5.0495
	Med	0	0	6.65×10^{-10}
	Worst	0	0	15.9679
F10	Avg	8.79×10^{-17}	5.55×10^{-16}	3.5×10^{-15}
	SD	0	0	4.15×10^{-14}
	Med	9.99×10^{-16}	5.55×10^{-15}	8.07×10^{-15}
	Worst	9.09×10^{-16}	5.55×10^{-15}	2×10^{-13}
F11	Avg	0	0.00074	0.090781
	SD	0	0.00234	0.19771
	Med	0	0	0.00000098
	Worst	0	0.0074	0.61623
F12	Avg	0.10412	4.71×10^{-32}	0.070837
	SD	0.43889	2.26×10^{-48}	0.020720

(continued)

Table I. Continued.

Functions		NOA	GTO	AHA
F13	Med	0.0000829	5.81×10^{-33}	0.086773
	Worst	2.148	5.81×10^{-33}	0.006228
	Avg	0.010807	1.35×10^{-32}	0.22513
	SD	0.026982	3.90×10^{-49}	0.08226
F14	Med	0.0072202	2.46×10^{-33}	0.35616
	Worst	0.061285	2.46×10^{-33}	0.43123
	Avg	0.998	0.998	1.5935
	SD	0	0	0.95823
F15	Med	0.998	0.998	0.99809
	Worst	0.998	0.998	2.9821
	Avg	0.0003828	0.000749	0.0008991
	SD	0.000238	0.000191	0.000331
F16	Med	0.0003075	0.000718	0.0007456
	Worst	0.0010602	0.00122	0.0014997
	Avg	-1.03161	-1.03	-1.0316
	SD	0	0	0.000016
F17	Med	-2.14272	-1.03	-2.1427
	Worst	-2.14272	-1.03	-2.1427
	Avg	0.40890	0.398	0.39898
	SD	0	0	0.0011636
F18	Med	0.40890	0.409	0.40946
	Worst	0.40890	0.398	0.40126
	Avg	2	2	2
	SD	0	2.96×10^{-16}	0.0000396
F19	Med	2	2	2
	Worst	2	2	2.0001
	Avg	-4.9739	-4.97	-4.9651
	SD	0	9.47×10^{-17}	0.0007109
F20	Med	-4.9719	-4.97	-4.9656
	Worst	-4.9719	-4.97	-4.964
	Avg	-3.2863	-3.32	-2.8029
	SD	0.057431	4.68×10^{-16}	0.38047
F21	Med	-3.322	-3.32	-3.0014
	Worst	-3.2031	-3.32	-1.9211
	Avg	-10.1532	-10.1	-3.0066
	SD	0	0.078	2.2011
F22	Med	-10.1532	-10.2	-3.1737
	Worst	-10.1532	-9.91	-0.4982
	Avg	-10.4029	-10.4	-4.1502
	SD	2.29×10^{-16}	2.43×10^{-16}	2.2208
F23	Med	-10.4029	-10.4	-4.707
	Worst	-10.4029	-10.4	-0.90936
	Avg	-10.5364	-8.45	-4.4381
	SD	1.78×10^{-15}	3.43	0.97997
	Med	-10.5364	-10.5	-4.6828
	Worst	-10.5364	-1.86	-2.8115

Avg: average; SD: standard deviation; Med: median; worst: worst of the best-so-far solution; NOA: nutcracker optimizer algorithm; GTO: gorilla troops optimization; AHA: artificial hummingbird algorithm.

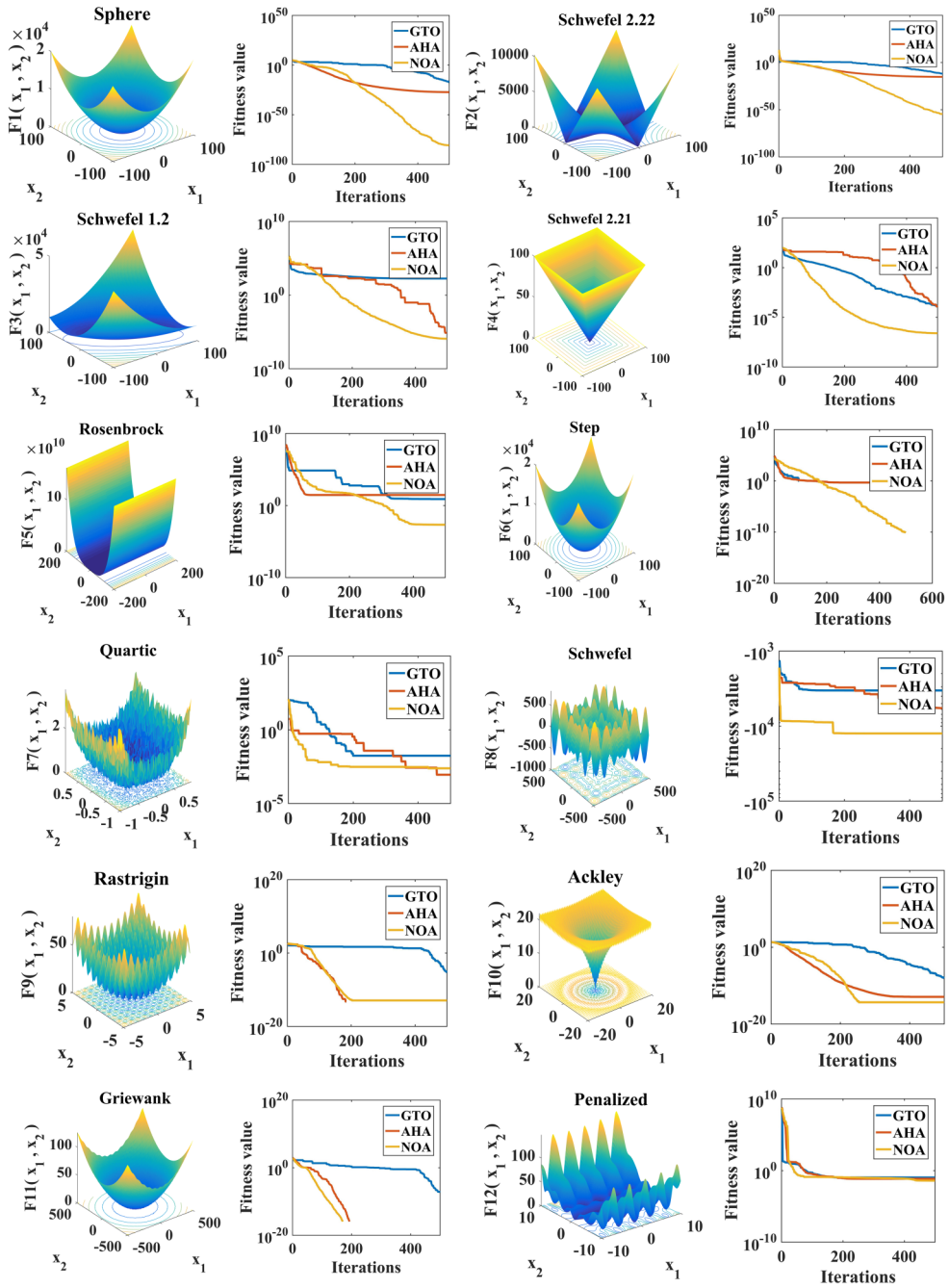


Figure I. Benchmark function representation and convergence profile of NOA, GTO, and AHA. NOA: nutcracker optimizer algorithm; GTO: gorilla troops optimization; AHA: artificial hummingbird algorithm. (continued)

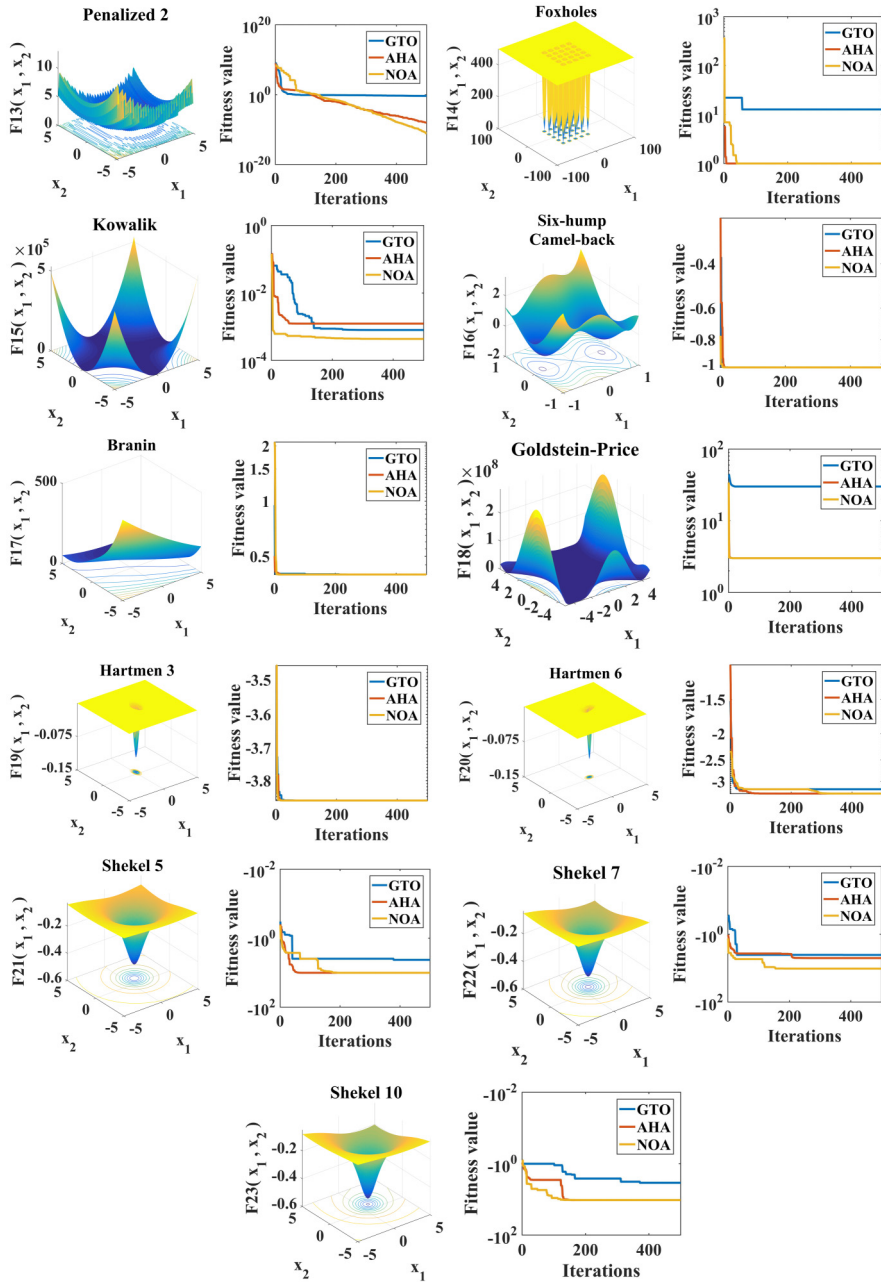


Figure I. Continued.

NOA to solve the CM problem, the same problem has also been solved with other recent well-known optimization techniques such as gorilla troops optimization (GTO), and artificial hummingbird algorithm (AHA). These techniques are applied in the same environment, enabling a fair comparison among different optimization methods for solving the CM problem.

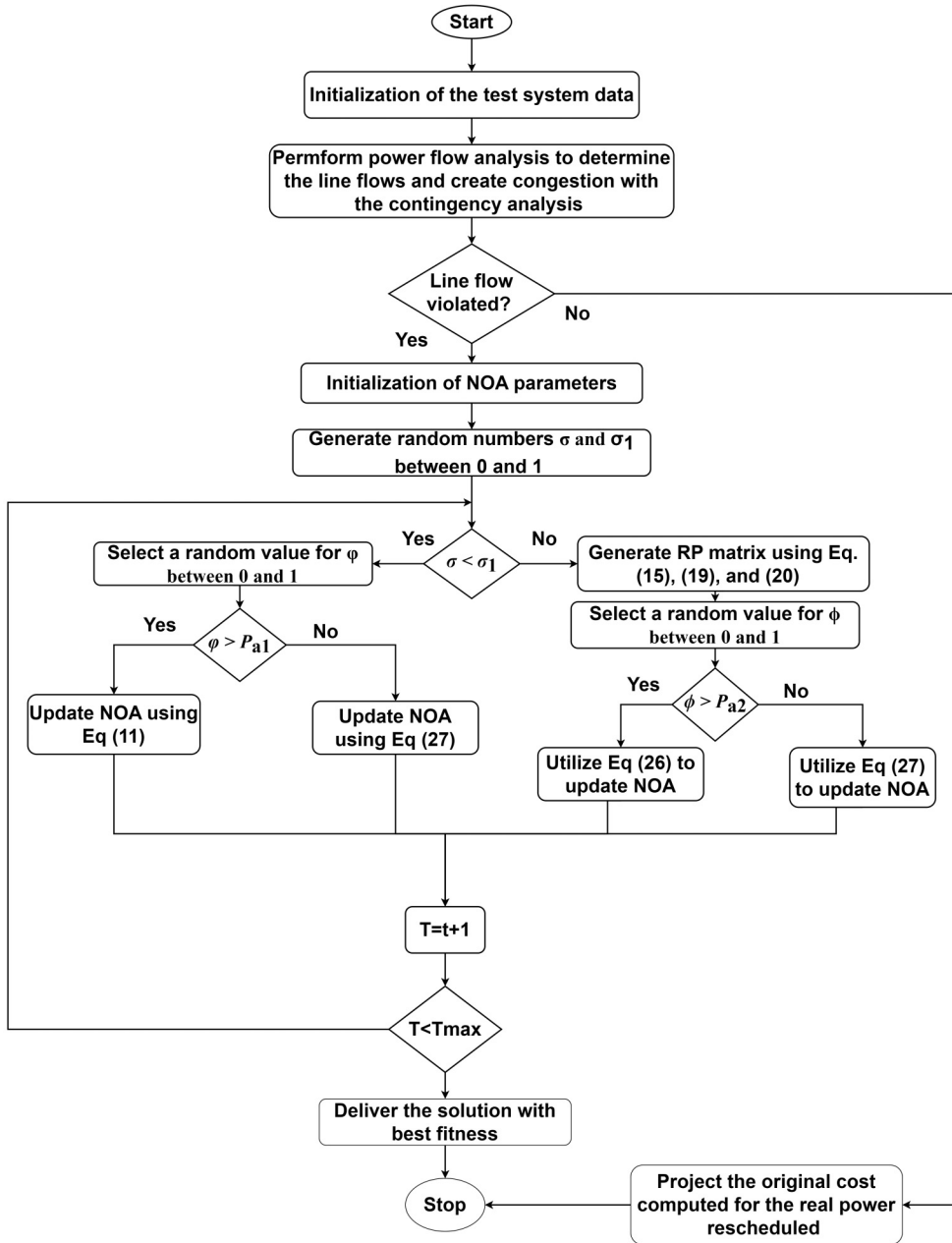


Figure 2. Flowchart for CM with NOA.
 NOA: nutcracker optimizer algorithm; CM: congestion management

The software used in this study is MATLAB 2016a and implemented on a system with an Intel Core i7 processor running at a clock speed of 2.4 GHz and equipped with 8 GB of RAM. Table 3 provides specific information about the simulated cases conducted on the test systems. In this

Table 2. Computational complexity time (NOA) in seconds.

Dimension (D)	T_0	T_1	T_2	$(T_2 - T_1)/T_0$
20	0.7539	7.8295	38.1602	34.3647
40	0.7539	44.3275	107.3527	75.1853
50	0.7539	106.2573	214.6285	132.5194

Table 3. Test cases considered for the congestion management (CM) problem.

Cases	Test system	Contingency scenario considered
1	IEEE 30-bus system (Sharma et al., 2018)	Tripping of lines 1 and 2
2	IEEE 118-bus system (Dash and Mohanty, 2015)	Tripping of lines 8–5 and load increment to 57% at buses 11–20

Table 4. Line power flow details for the congested line.

	Congested lines	Power flow (MW)	Power flow limit (MW)	Excess power flow (MW)	% overload
Outage of lines 1 and 2	1–3	147.46	130	17.46	13.43
	6–8	136.29	130	6.29	4.84

research, line overloads have been created considering two cases, firstly, by decreasing the power flow capacity of the capacity of the lines, and secondly, by simulating line outage(s) for contingency purposes.

To find the optimal parameter values, multiple trial runs have been conducted for solving the CM problem on all three test systems under study. The best results obtained from these trials are presented. Through these trial runs, the population size of 40 has been considered to be sufficient for the CM problem in this particular study.

IEEE 30-bus system

The modified IEEE 30-bus test system has been considered for the evaluation of the CM problem. It consists of 41 transmission channels with six generator buses and 24 load buses. The configuration of this system is depicted in Figure 2. The test case that has been considered for the IEEE 30-bus system is listed in Table 3. The details of the congested power flow scenario are given in Table 4.

In this case, the congestion has been created by an outage of line 1, between buses 1 and 2 (Figure 3). This leads to congestion in line 2 (connecting buses 1 and 3) and line 4 (connecting buses 6 and 8) and is represented in Table 4. To ensure secure functioning, counteractive measures are necessary to relieve these overloaded lines. The NOA has been employed to minimize the congestion cost, with the optimal generator output. The congestion costs obtained using the NOA are presented in Table 5. These values are then compared with results from literature, such as PSO (Kamaraj, 2011), RSM (Kamaraj, 2011), SA (Kamaraj, 2011), FPA (Verma and Mukherjee, 2016b), CBA (Verma and Mukherjee, 2016b), ALO (Verma and Mukherjee, 2016b), TLBO (Verma et al., 2018) as well as recent algorithms like GTO, AHA. The optimal total congestion cost obtained through the NOA-based approach is determined to be 476.84 \$/h.

Table 5. Comparative outcomes for IEEE 30 bus system with NOA.

	RSM (Kamaraj, 2011)	PSO (Kamaraj, 2011)	SA (Kamaraj, 2011)	FPA (Verma and Mukherjee, 2016b)	CBA (Verma and Mukherjee, 2016b)	ALO (Verma and Mukherjee, 2016b)	TLBO (Verma et al., 2018)	GTO [solved]	AHA [solved]	NOA [proposed]
Congestion cost (\$/h)	716.25	538.95	719.86	519.62	482.02	480.04	494.66	526.79	503.15	476.84
Best congestion cost (\$/h)	NR ^a	NR ^a	NR ^a	NR ^a	NR ^a	NR ^a	NR ^a	526.79	503.15	476.84
Worst congestion cost (\$/h)	NR ^a	NR ^a	NR ^a	NR ^a	NR ^a	NR ^a	NR ^a	796.53	686.48	510.84
Line (1–3) power flow (post CM)	129.78	129.97	129.51	129.60	129.97	129.5	130.00	129.40	129.57	129.40
Line (6–8) power flow (post CM)	120.60	120.62	120.35	120.58	120.79	120.79	120.78	120.38	120.65	120.03
ΔP_1 (MW)	-8.808	-8.61	-9.076	-9.127	-8.694	-9.0880	-8.5876	-9.180	-8.975	-7.7642
ΔP_2 (MW)	2.647	10.40	3.133	14.14	13.917	15.0668	12.9855	12.19	2.634	10.4476
ΔP_3 (MW)	2.953	3.03	3.234	0.206	0.016	0.0198	0.4598	0.206	3.08	0.3487
ΔP_4 (MW)	3.063	0.02	2.968	0.0188	0.109	0.0001	0.7289	0.018	1.869	0.6178
ΔP_5 (MW)	2.913	0.85	2.954	0.189	0.349	0.0002	0.0093	0.908	2.471	0.0074
ΔP_6 (MW)	2.952	0.01	2.443	1.013	0.317	0.0001	0.3988	1.117	1.082	0.2877
Total amount (MW)	23.33	22.93	23.80	24.703	23.402	24.1552	23.169	23.619	20.111	19.4734

NOA: nutcracker optimizer algorithm; GTO: gorilla troops optimization; AHA: artificial hummingbird algorithm; PSO: particle swarm optimization; FPA: flower pollination algorithm; RSM: random search method; SA: simulated Annealing; CBA: chaotic bat algorithm; ALO: ant lion optimizer; TLBO: teaching learning based optimization.
^aNR: not reported.

Representation of the comparative congestion costs is depicted in Figure 4. Figure 5 illustrates the real power rescheduling for different generators achieved by the comparative algorithms. The convergence profiles of GTO, AHA, and NOA, are presented in Figure 6. The iterative values for 30 runs with 500 iterations and the box plot are given in Figures 7 and 8.

Additionally, the total system loss is reduced to 12.047 MW after CM, compared to the initial value of 16.023 MW during congestion. The bus voltages after CM using the NOA approach are shown in Figure 9, where it is evident that all bus voltages remain within acceptable limits.

Statistical test for NOA on IEEE 30-bus system. To assess the effectiveness and resilience of the proposed NOA, an extensive examination has been conducted on the obtained results. This involved

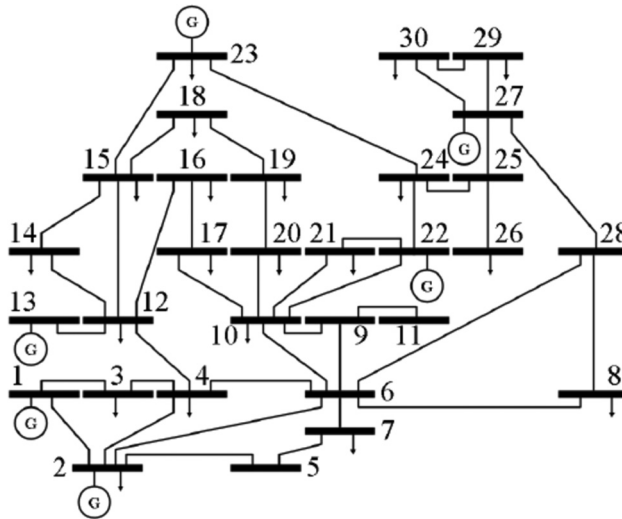


Figure 3. Single line representation of IEEE 30-bus system (Verma et al., 2018).

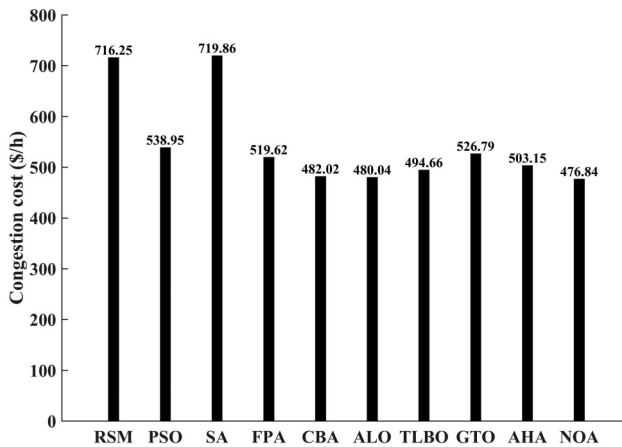


Figure 4. Comparative congestion cost with nutcracker optimizer algorithm (NOA) and other optimization algorithms.

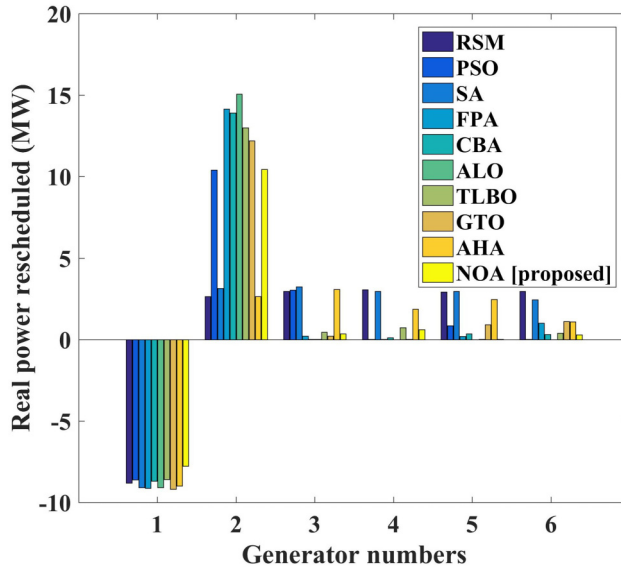


Figure 5. Comparative representation of the real power rescheduled with the optimization algorithms.

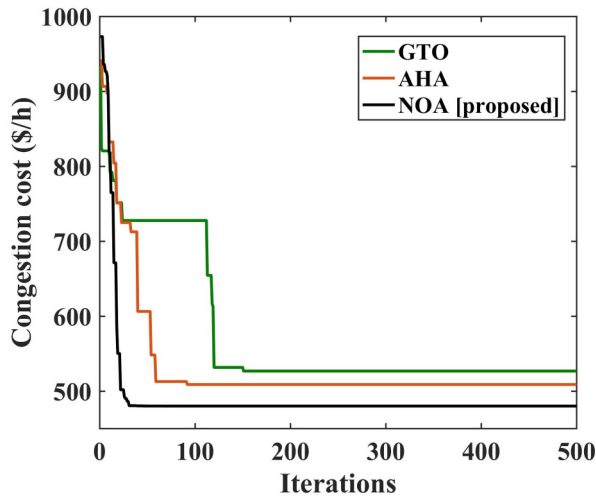


Figure 6. Convergence characteristics of nutcracker optimizer algorithm (NOA) and other optimization algorithms.

running all three optimization algorithms 30 times across various population sizes (number of search agents). According to Derrac et al. (2011), the authors recommended employing several non-parametric statistical tests within the realm of computational intelligence. Table 6 shows the cases with the best fitness function values. Notably, the NOA yielded the best result when utilizing 40 search agents. Table 7 presents the minimum, maximum, mean, and standard deviations of fitness function values obtained with GTO, AHA, and NOA when using 40 search agents.

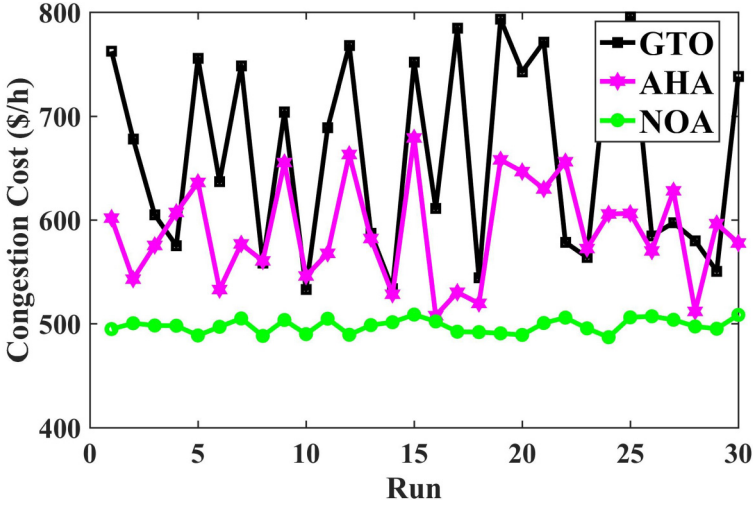


Figure 7. Fitness function values for 30 runs with 500 iterations (IEEE 30 bus).

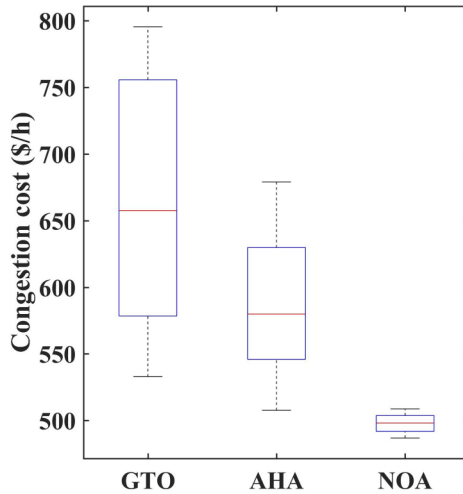


Figure 8. Box plot for 30 trail runs (IEEE 30 bus).

Furthermore, statistical analyses including Friedman, and Quade tests have been conducted to validate the optimization algorithms. Let H_0 denote the hypothesis stating no difference among the three methods, while H_1 represents the alternative hypothesis suggesting differences (Sheskin, 2003). A significance level of $\alpha=0.05$ has been chosen. Table 8 presents the recorded p -values from Wilcoxon’s paired sign rank test. The symbols $+/-/\sim$ indicate whether the proposed NOA outperforms, underperforms, or is approximately equal to the compared algorithm, respectively. A p -value < 0.05 for all test cases refutes the null hypothesis, affirming the validity of Wilcoxon’s signed-rank test for the proposed algorithm (Sheskin, 2003).

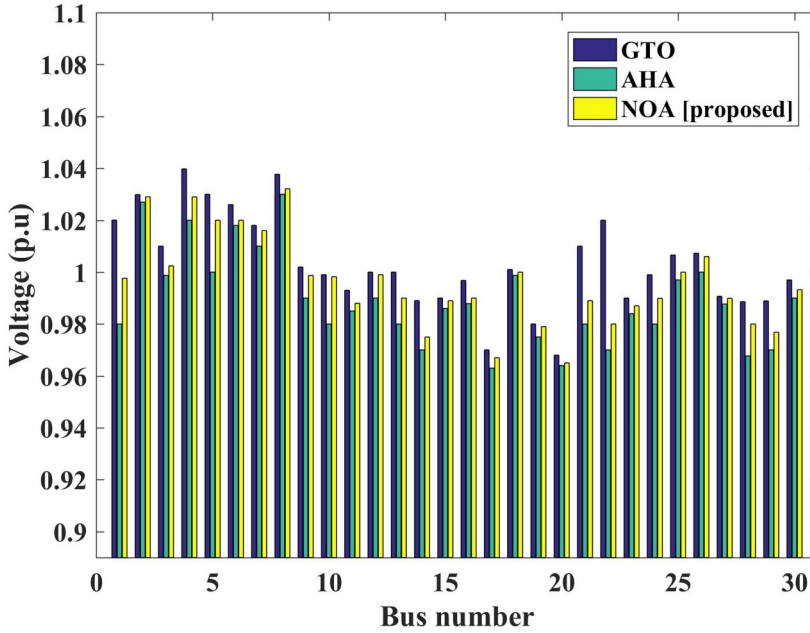


Figure 9. Comparative bus voltage with nutcracker optimizer algorithm (NOA) and other optimization techniques.

Table 6. The fitness function value is delivered by the optimization algorithm for different search agents.

Algorithms	Search agents			
	20	30	40	50
GTO	531.68	528.90	526.79	524.25
AHA	509.16	507.99	503.15	502.17
NOA	483.36	479.56	476.84	474.75

NOA: nutcracker optimizer algorithm; GTO: gorilla troops optimization; AHA: artificial hummingbird algorithm.

Table 7. Fitness function values delivered by GTO, AHA, and NOA for 40 search agents

Algorithms	Min	Max	Avg	SD
GTO	526.79	796.53	662.905	12.6942
AHA	503.15	686.48	589.049	9.0678
NOA	476.84	510.84	497.966	4.7358

Avg: average; SD: standard deviation; Med: median; worst: worst of the best-so-far solution; NOA: nutcracker optimizer algorithm; GTO: gorilla troops optimization; AHA: artificial hummingbird algorithm.

Analysis of variance relies on the principle of total variance. This approach involves breaking down the observed variance in a specific variable into segments attributed to various sources of variation. The critical *F*-value is determined with the chosen significance level ($\alpha = 0.05$). If the

Table 8. *p*-values for the optimization algorithm.

Algorithm	<i>p</i> -value	+/-/~
GTO versus NOA	1.7344×10^{-6}	+
AHA versus NOA	1.9209×10^{-6}	+

NOA: nutcracker optimizer algorithm; GTO: gorilla troops optimization; AHA: artificial hummingbird algorithm.

Table 9. Analysis of variance for the optimization algorithms.

Source of variation	Sum of square	Degrees of freedom	Mean square	<i>F</i> -ratio	5% <i>F</i> -limit
Between techniques	3.5257×10^7	5-1 = 4	9.0420×10^6	14.6751	$F(4, 25) = 2.8696$
Within techniques	1.3718×10^7	30-5 = 25	5.7279×10^5		

Table 10. Representation of average error for GTO, AHA, and NOA.

Search agents	GTO	AHA	NOA
20	23.2889	32.43046	2.74084
30	45.87211	13.86326	1.69437
40	38.75376	2.654998	1.49064
50	28.10499	26.79083	2.76185

NOA: nutcracker optimizer algorithm; GTO: gorilla troops optimization; AHA: artificial hummingbird algorithm.

Table 11. Friedman test analysis data.

Search agents	Friedman ranks		
	GTO	AHA	NOA
20	4	2	1
30	4	2	1
40	4	2	1
50	4	2	1
Avg. Rank	4	2	1
<i>F</i> -statistic	16		
<i>P</i> -value	0.0020		

NOA: nutcracker optimizer algorithm; GTO: gorilla troops optimization; AHA: artificial hummingbird algorithm.

calculated *F*-ratio exceeds the critical *F*-limit, the null hypothesis is rejected. Additionally, Table 9 indicates that the computed *F*-value falls below the tabulated *F*-value at a 5% significance level, where the degrees of freedom are specified as 4 and 25.

To conduct the Friedman and Quade tests, initially, an average error table is highlighted in Table 10. Subsequently, Friedman ranks and the *F*-statistic (also known as the χ^2 value) are computed and presented in Table 11. The method with the lowest rank is deemed superior, clearly indicating the efficacy of NOA. The computed χ^2 value of 16 from Table 11 exceeds

Table 12. Representation of Quade test analysis for GTO, AHA, and NOA.

Search agents	Quade ranks		
	GTO	AHA	NOA
20	4	-8	-6
30	4	-2	-3
40	4	-6	-2
50	4	2	-1
Sum Rank	4	2	-12
Q-statistic	15		
F-value	$1.3970 \times 10^{-0.3}$		

NOA: nutcracker optimizer algorithm; GTO: gorilla troops optimization; AHA: artificial hummingbird algorithm.

Table 13. Details of congested lines (118 bus).

	Congested lines (MW)	Power flow (MW)	Line limit (MW)	Excess power flow (MW)	% overload
Tripping of lines 8-5 with an increase in load at buses 11-20 by 57%	16-17	209.14	175	34.14	12.83
	30-17	568.73	500	13.16	37.6
	8-30	380.59	175	205.59	54.01

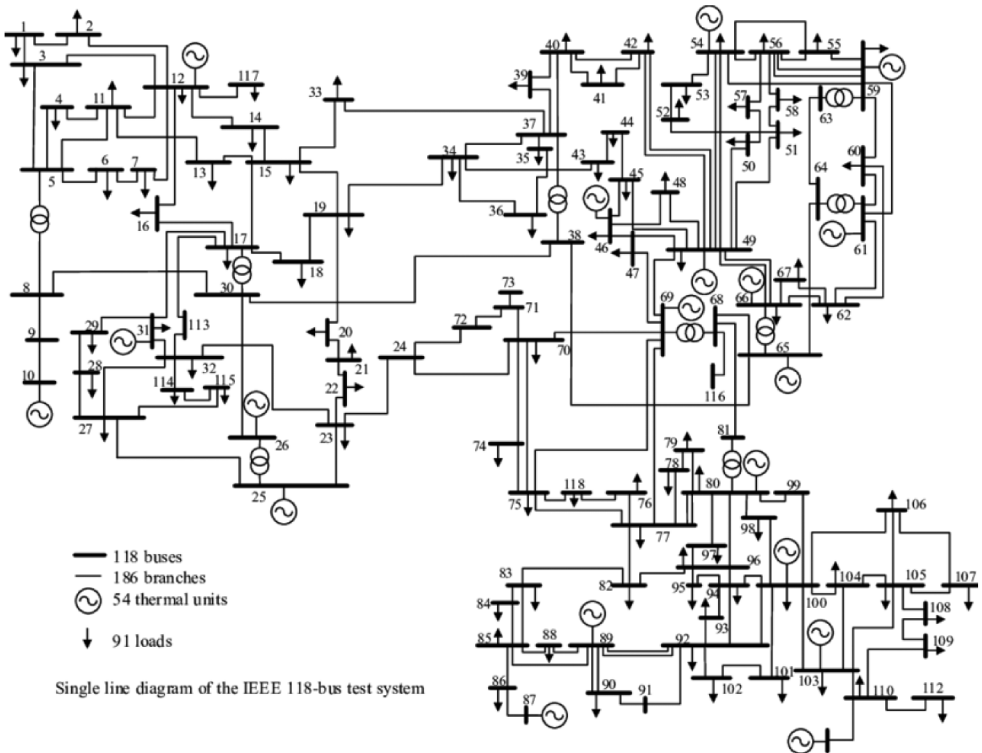


Figure 10. Single line diagram of 118-bus system (Wang et al., 2022).

Table 14. Comparative outcomes for IEEE 118-bus system with NOA.

	RCGA (Kamaraj, 2011)	EP (Kamaraj, 2011)	DE (Kamaraj, 2011)	HPSO (Verma and Mukherjee, 2016b)	PSO (Verma and Mukherjee, 2016b)	CBA (Verma and Mukherjee, 2016b)	ALO (Verma et al., 2018)	GTO [solved]	AHA [solved]	NOA [proposed]
Congestion cost (\$/h)	17.693	42.886	16,080	17,365	17,742	15,724	15,448	1528.07	1438.90	1389.56
Best congestion cost (\$/h)	NR ^a	NR ^a	NR ^a	NR ^a	NR ^a	NR ^a	NR ^a	1528.07	1438.90	1389.56
Worst congestion cost (\$/h)	NR ^a	NR ^a	NR ^a	NR ^a	NR ^a	NR ^a	NR ^a	2100.48	1845.78	1420.56
Lines (16 and 17) power flow (post CM)	174.26	173.89	174.37	174.62	174.15	174.09	174.20	174.23	174.87	173.18
Lines (30–17) power flow (post CM)	499.09	498.14	496.88	495.42	496.09	499.36	497.94	496.36	497.30	495.42
Line (8–30) power flow (post CM)	174.68	174.54	174.20	174.59	174.82	174.31	174.76	174.48	174.00	174.02
ΔP_{G1}	26.274	38.11	6.4705	11.59	24.502	0.0124	0.0177	13.317	4.8963	11.934
ΔP_{G2}	0	0	0	0	0	0.0455	0.0362	0.0087	0.0051	9.6558
ΔP_{G3}	31.422	63.06	12.295	6.568	1.0259	0.1476	17.266	0.7567	0.0035	1.665
ΔP_{G4}	11.349	-7.48	-0.056	-0.046	1.3148	-0.0261	-0.0031	83.455	-0.0005	0
ΔP_{G5}	-219.3	-200.6	-208.1	-207.7	-21.82	-207.8	-207.83	-0.2312	0.0237	0
ΔP_{G6}	101.42	48.58	105.32	80.126	105.32	105.31	105.32	1.4716	0.0001	113.40
ΔP_{G7}	0	0	0	0	0	0.0086	0.002	5.777	0.0452	101.12
ΔP_{G8}	0.0029	49.17	1.9946	6.0059	16.815	-0.0081	4.6839	22.78	0.0023	0
ΔP_{G9}	8.0582	64.056	1.2884	-0.239	23.665	0.0095	2.597	-0.125	0.2974	4.409
ΔP_{G10}	0	0	0	0	0	0.003	0.0042	3.0727	0.0223	15.742

(continued)

Table 14. Continued.

	RCGA (Kamaraj, 2011)	EP (Kamaraj, 2011)	DE (Kamaraj, 2011)	HPSO (Verma and Mukherjee, 2016b)	PSO (Verma and Mukherjee, 2016b)	CBA (Verma and Mukherjee, 2016b)	ALO (Verma et al., 2018)	GTO [solved]	AHA [solved]	NOA [proposed]
ΔP_{G11}	114.69	121.51	49.697	121.51	121.51	0.1359	0.0915	1.5325	0.0019	0
ΔP_{G12}	116.31	25.918	113.29	108.06	116.31	0.1555	28.186	2.5903	0.0276	0
ΔP_{G13}	7.4155	85.370	0.8125	10.752	3.0092	0.0074	-0.0024	3.7627	0.1654	-10.03
ΔP_{G14}	-0.0019	32.857	2.1836	-0.536	0.0177	0.0041	0.0678	12.6412	0.2261	11.165
ΔP_{G15}	28.095	31.616	89.669	11.254	8.8665	89.701	89.765	0.4368	46.1738	-0.5718
ΔP_{G16}	1.7508	39.071	0.7819	0.0731	7.1475	0.0006	0.0025	-0.4615	0.0002	-207.3
ΔP_{G17}	0.0004	37.552	-0.041	-0.394	0.4916	0.0884	0.004	3.0092	0.0006	104.93
ΔP_{G18}	0	0	0	0	0	0.0082	0.0426	0.0177	2.3777	0.8256
ΔP_{G19}	0	0	0	0	0	0.0022	0.0036	8.8665	116.12	0.0023
ΔP_{G20}	1.7478	89.001	-0.089	4.3096	6.0792	0	0.1504	7.1475	0.0001	1.6977
ΔP_{G21}	18.528	96.075	102.85	77.661	19.359	22.358	25.114	0.4916	0.2949	2.1221
ΔP_{G22}	33.426	93.828	7.3786	72.901	36.798	0.4626	8.6749	28.186	69.115	8.3874
ΔP_{G23}	0	0	0	0	0	0.0236	-0.0141	-0.0024	0.0140	13.317
ΔP_{G24}	0	0	0	0	0	0.0003	0.0059	0.0678	-0.0273	0.0087
ΔP_{G25}	0	0	0	0	0	9.0881	17.745	89.765	-0.0004	0.7567
ΔP_{G26}	0	0	0	0	0	10.296	8.1664	0.0025	0.9068	-0.0018
ΔP_{G27}	0	0	0	0	0	0.0101	-0.0024	0.004	0.0748	28.095
ΔP_{G28}	0	0	0	0	0	3.3333	33.28	0.0426	42.198	1.7508
ΔP_{G29}	0	0	0	0	0	14.779	9.1758	0.0036	0.0004	0.0004
ΔP_{G30}	0	-450.9	4.904	0.6525	10.702	1.1904	0.6717	0.1504	0.0052	0
ΔP_{G31}	0	0	0	0	0	0.0015	0.0173	25.114	0.0001	0
ΔP_{G32}	0	0	0	0	0	-0.0016	0.0032	8.6749	16.815	1.7478
ΔP_{G33}	0	0	0	0	0	0.3726	0.0218	-0.0141	23.665	18.528
ΔP_{G34}	0	0	0	0	0	0.2975	0.0024	48.58	0	33.426
ΔP_{G35}	0	0	0	0	0	0.0656	0.1945	0	121.51	10.752
ΔP_{G36}	0	0	0	0	0	0.0048	0.0013	49.17	116.31	-0.536
ΔP_{G37}	0	0	0	0	0	137.81	39.667	64.056	3.0092	11.254
ΔP_{G38}	0	0	0	0	0	0.0491	0.0372	0	0.0177	0.0731

(continued)

Table 14. Continued.

	RCGA (Kamaraj, 2011)	EP (Kamaraj, 2011)	DE (Kamaraj, 2011)	HPSO (Verma and Mukherjee, 2016b)	PSO (Verma and Mukherjee, 2016b)	CBA (Verma and Mukherjee, 2016b)	ALO (Verma et al., 2018)	GTO [solved]	AHA [solved]	NOA [proposed]
ΔP_{G39}	0	0	0	0	0	0.0145	2.7964	121.51	8.8665	-0.394
ΔP_{G40}	0	0	0	0	0	-0.003	0.0031	25.918	7.1475	0
ΔP_{G41}	0	0	0	0	0	0.0317	0.0033	85.370	0.4916	0
ΔP_{G42}	0	0	0	0	0	0.0835	0.0151	32.857	0.004	4.3096
ΔP_{G43}	0	0	0	0	0	0.0413	0.4569	1.2884	0.0426	77.661
ΔP_{G44}	0	0	0	0	0	0.0055	0.0073	0	0.0036	72.901
ΔP_{G45}	0	0	0	0	0	0.0035	0.196	49.697	0.1504	4.9421
ΔP_{G46}	719.8998	1574.9	707.3281	720.4816	717.7839	24.224	3.2218	113.29	205.114	71.938
ΔP_{G47}	0	0	0	0	0	0.0019	-0.0015	0.8125	8.6749	0.9656
ΔP_{G48}	0	0	0	0	0	-0.012	-0.0013	2.1836	-0.0141	-0.092
ΔP_{G49}	0	0	0	0	0	0.0096	0.0039	89.669	0.0059	1.53
ΔP_{G50}	0	0	0	0	0	0.0056	0.0012	0.7819	17.745	0.0023
ΔP_{G51}	0	0	0	0	0	102.026	100.433	116.31	8.1664	0.3837
ΔP_{G52}	0	0	0	0	0	0.0277	-0.0045	7.4155	-0.0024	22.78
ΔP_{G53}	0	0	0	0	0	0.0032	7.3507	-0.0019	33.28	-0.125
ΔP_{G54}	0	0	0	0	0	-0.0001	0.0009	28.095	9.1758	3.0727
Total amount (MW)	1439.6913	2149.654	1414.5492	1440.8597	1242.5373	730.1113	713.3677	1160.9855	863.2383	986.302

RCGA: Real coded GA; DE: differential evolution; HPSO: hybrid PSO; CBA: chaotic bat algorithm; ALO: ant lion optimizer.
 NOA: nutcracker optimizer algorithm; GTO: gorilla troops optimization; AHA: artificial hummingbird algorithm; PSO: particle swarm optimization.
^aNR: not reported.

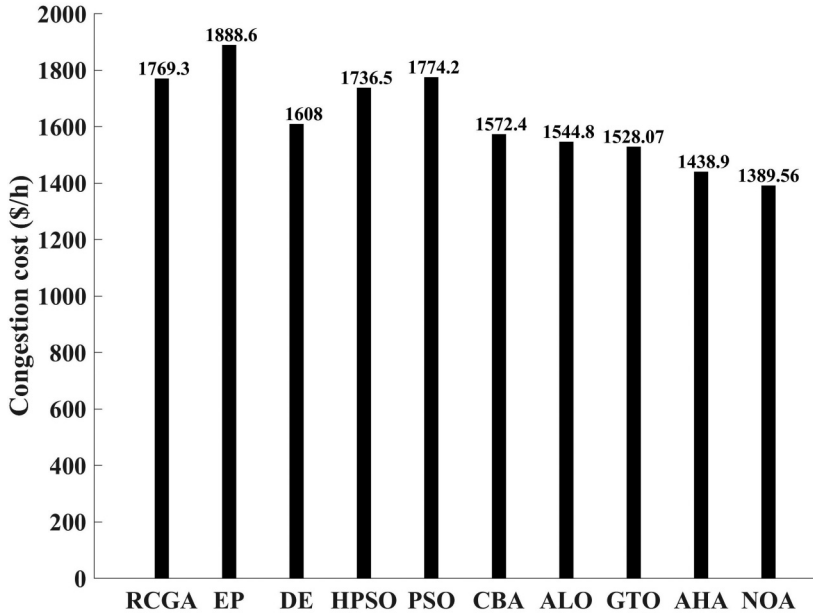


Figure 11. Comparative congestion cost with nutcracker optimizer algorithm (NOA) and other optimization algorithms.

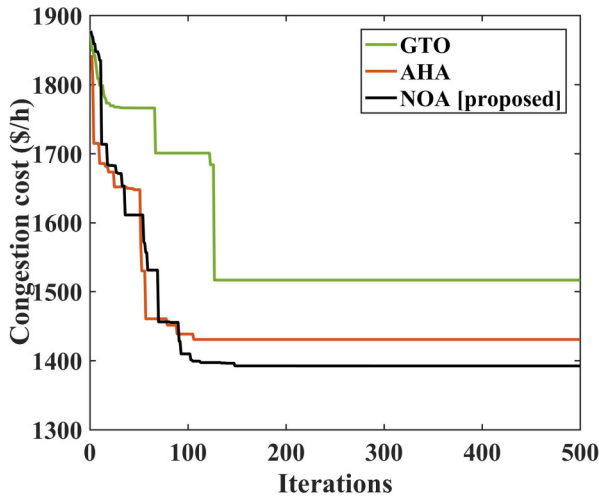


Figure 12. Convergence characteristics of nutcracker optimizer algorithm (NOA) and other optimization algorithms.

the critical value, and the resulting p -value of 0.0030, being < 0.05 , leads to the rejection of the null hypothesis. This confirms the presence of significant disparities among the methods employed.

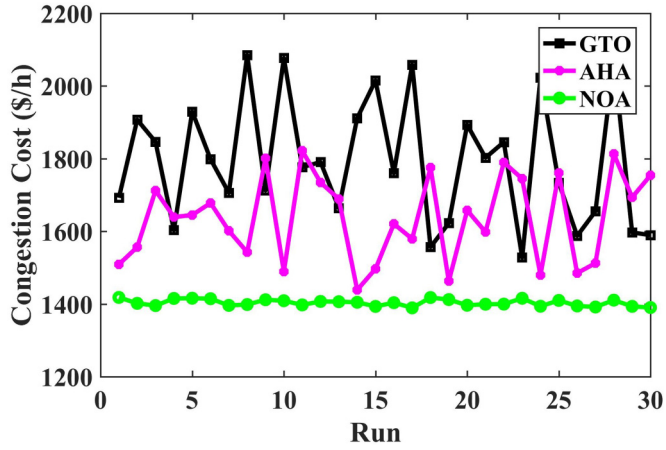


Figure 13. Fitness function values for 30 runs with 500 iterations (IEEE 118 bus).

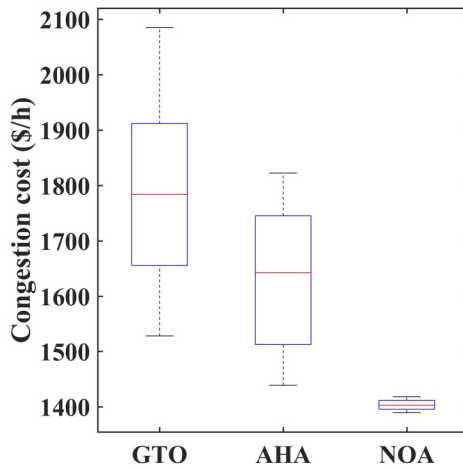


Figure 14. Figure 8 box plot for 30 trail runs (IEEE 118 bus).

Table 15. Fitness function value delivered by the optimization algorithm for different search agents (118 bus).

Algorithms	Search agents			
	20	30	40	50
GTO	1536.47	1534.09	1528.07	1524.27
AHA	1446.61	1442.17	1438.90	1436.79
NOA	1396.36	1391.56	1389.56	1380.58

NOA: nutcracker optimizer algorithm; GTO: gorilla troops optimization; AHA: artificial hummingbird algorithm.

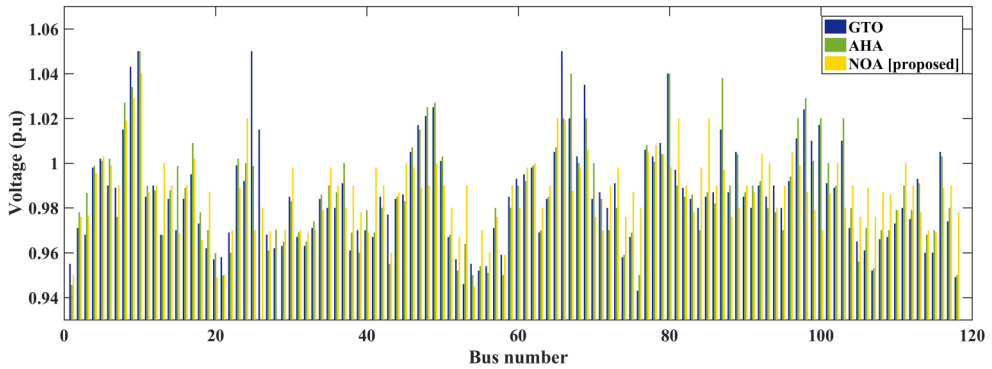


Figure 15. Comparative bus voltage with nutcracker optimizer algorithm (NOA) and other optimization techniques.

Table 16. Fitness function values delivered by GTO, AHA, and NOA for 40 search agents (118 bus).

Algorithms	Min	Max	Avg	SD
GTO	1528.07	2100.48	1602.05	14.9342
AHA	1438.90	1845.78	1549.49	12.3857
NOA	1389.56	1420.56	1436.66	3.8469

NOA: nutcracker optimizer algorithm; GTO: gorilla troops optimization; AHA: artificial hummingbird algorithm.

Table 17. *P*-values for the optimization algorithm (118 bus).

Algorithm	<i>p</i> -value	+/-/~
GTO versus NOA	1.6723×10^{-6}	+
AHA versus NOA	1.7318×10^{-6}	+

NOA: nutcracker optimizer algorithm; GTO: gorilla troops optimization; AHA: artificial hummingbird algorithm.

Table 18. Analysis of variance for the optimization algorithms (118 bus)

Source of variation	Sum of square	Degrees of freedom	Mean square	<i>F</i> -ratio	5% <i>F</i> -limit
Between techniques	3.6319×10^7	5-1 = 4	8.1479×10^6	15.5348	$F(4, 25) = 3.4186$
Within techniques	1.2187×10^7	30-5 = 25	4.5547×10^5		

Similar trends are evident in the Quade test results presented in Table 12, where NOA achieved the lowest rank. The calculated *Q*-statistic value of 15 surpasses the critical value referenced by Sheskin (2003), and the resulting *p*-value of 1.9209×10^{-6} , being < 0.05 , supports the rejection of the null hypothesis H_0 . This reinforces the effectiveness of NOA.

Table 19. Representation of average error for GTO, AHA, and NOA (118 bus).

Search agents	GTO	AHA	NOA
20	34.39910	43.54157	3.85195
30	56.98322	24.97437	2.70548
40	49.86487	3.765009	2.50175
50	39.215010	37.80194	3.87296

NOA: nutcracker optimizer algorithm; GTO: gorilla troops optimization; AHA: artificial hummingbird algorithm.

Table 20. Representation of FRIEDMAN test analysis for GTO, AHA, and NOA (118 bus).

Search agents	Friedman ranks		
	GTO	AHA	NOA
20	3	2	1
30	3	2	1
40	3	2	1
50	3	2	1
Avg. Rank	3	2	1
F-statistic	15		
P-value	0.0040		

NOA: nutcracker optimizer algorithm; GTO: gorilla troops optimization; AHA: artificial hummingbird algorithm.

Table 21. Representation of Quade test analysis for GTO, AHA, and NOA (118 bus).

Search agents	Quade ranks		
	GTO	AHA	NOA
20	4	-7	-7
30	4	-3	-2
40	4	-5	-3
50	4	3	-2
Sum Rank	16	-12	-14
Q-statistic	14		
F-value	$1.2851 \times 10^{-0.3}$		

NOA: nutcracker optimizer algorithm; GTO: gorilla troops optimization; AHA: artificial hummingbird algorithm.

IEEE 118-bus system

This test framework consists of 54 buses as generator buses, 186 transmission lines, and 64 load buses. The network topology for this test system can be found in Figure 10.

In this test system, contingency is established with the tripping of lines 8–5 and increasing the load demand by 1.57 times. Congested lines detail have been represented in Table 13. The NOA has been employed to settle the CM problem and obtain the solution. The detail of the solutions achieved with the NOA has been highlighted in Table 14. It can be seen that the line flows have been reduced below the maximum limits with the NOA and other competitive

optimization algorithms. The congestion cost and the real power rescheduled by the NOA, and other recent algorithms are summarized in Table 14. It is observed that the application of NOA and generator rescheduling have relieved the overloaded lines achieving a congestion cost of 1389.56 \$/h, which is comparatively lower than the cost achieved with other techniques.

The congestion cost is represented in Figure 11. Convergence of the fitness function based on the NOA for this case is depicted in Figure 12. System loss before CM was 247.968 MW, whereas post CM it has been reduced to 168.539 MW. Furthermore, tests have shown that NOA consistently provides the best optimal solution even for large systems. The iterative values for 30 runs with 500 iterations and the box plot are given in Figures 13 and 14. The bus voltages obtained post-CM are represented in Figure 15, demonstrating that the voltages are within normal specified limits.

Statistical test for NOA on IEEE 118-bus system. The fitness obtained with GTO, AHA, and NOA is highlighted in Table 15. Notably, the NOA yielded the best result when utilizing 40 search agents. Table 16 presents the minimum, maximum, mean, and standard deviations of fitness function values. Various statistical analyses, including Wilcoxon's signed-rank test, Friedman, and Quade tests, were undertaken to assess the algorithms. H_0 represents the hypothesis asserting no distinctions among the three methods, while H_1 suggests otherwise (Verma and Mukherjee, 2016a). A significance level of $\alpha=0.05$ was selected for the analyses. The p -values obtained from Wilcoxon's paired sign rank test are presented in Table 17. The symbols $+/-/\sim$ indicate whether the proposed NOA performs better, worse, or comparably to the compared algorithm, respectively. A p -value < 0.05 across all test cases negates the null hypothesis, confirming the credibility of Wilcoxon's signed-rank test for the proposed algorithm (Verma and Mukherjee, 2016a).

Additionally, as depicted in Table 18, the computed F -value for both systems falls below the tabulated F -value at a 5% significance level, with degrees of freedom specified as 4 and 25. In conducting the Friedman and Quade tests, an average error table is established in resembling Table 19. Subsequently, Friedman ranks, and the F -statistic (also referred to as the χ^2 value) are computed and presented in Table 20. The method achieving the lowest rank is deemed superior, thereby highlighting the effectiveness of NOA. The calculated χ^2 value of 16 from Table 20 surpasses the critical value, and the resulting p -value of 0.0030, falling below 0.05, leads to the rejection of the null hypothesis, indicating significant disparities among the employed methods. Similar patterns are observable in the Quade test outcomes showcased in Table 21, where NOA secures the lowest rank. The calculated Q -statistic value of 15 exceeds the referenced critical value by Verma and Mukherjee (2016a), and the resulting p -value of 1.9209×10^{-6} , being below 0.05, supports the rejection of null hypothesis H_0 , thus reinforcing the efficacy of NOA.

Conclusions

This research introduces a novel approach for power system CM within the power market, utilizing a generation rescheduling method. The contribution can be stated as the formulation of a novel CM model to minimize congestion costs through optimal rescheduling of generators' real power, utilizing NOA for determining optimal power rescheduling patterns. This model's efficacy is validated on power system standard test systems, IEEE 30 bus, and IEEE 118 bus. Comparative performance analysis is conducted, assessing congestion cost reduction, bus voltage profile improvement, and system losses, demonstrating the superiority of the proposed CM model with NOA over contemporary optimization techniques. The method employs a unique NOA and accounts for contingencies like line outages and sudden load variations. It aims to alleviate congestion in overloaded lines

by adjusting the power generation schedules while minimizing the congestion cost. The NOA technique has been successfully applied to IEEE 30- and IEEE 118-bus systems for CM purposes. Comparisons are made between the outcomes generated by the proposed NOA and various established algorithms documented in recent literature. Results indicate that the power rescheduled with NOA incurs lower congestion costs as compared to other similar techniques. Furthermore, applying CM reduces the overall system loss.

Consequently, the NOA offers a fresh and efficient approach to resolving power system CM challenges within a deregulated framework. Considering future approaches, the suggested approach for power system congestion management, employing NOA, has the potential for expansion towards optimizing power system operations, encompassing power dispatch and load scheduling strategies. It can also be utilized to examine the optimal positioning and control of power delivery from renewable energy systems and distributed generation, offering a comprehensive analysis of the proposed methodology.

Further, researchers dealing with large-scale power system issues might find the NOA a valuable optimization tool based on its demonstrated effectiveness. Research on power system transmission line congestion management using optimization techniques encounters several challenges. These include the complexity of power networks, data availability and accuracy issues, long computational times, the need for adaptable algorithms, and the integration of renewable energy sources. Overcoming these limitations is essential for enhancing the effectiveness and practicality of optimization approaches in real-world applications. Further, the researchers dealing with large-scale power system issues might find the NOA a valuable optimization tool based on its demonstrated effectiveness.


Declaration of conflicting interests

The author(s) declared no potential conflicts of interest with respect to the research, authorship, and/or publication of this article.

Funding

The author(s) received no financial support for the research, authorship, and/or publication of this article.

ORCID iD

Kaushik Paul  <https://orcid.org/0000-0002-4022-0038>

References

- Abdel-Basset M, Mohamed R, Jameel M, et al. (2023) Nutcracker optimizer: A novel nature-inspired metaheuristic algorithm for global optimization and engineering design problems. *Knowledge-Based Systems* 262: 110248.
- Agrawal A, Pandey SN, Srivastava L, et al. (2022) Hybrid deep neural network-based generation rescheduling for congestion mitigation in spot power market. *IEEE Access* 10: 29267–29276.
- Alavijeh NM, Steen D, Le AT, et al. (2024) Capacity limitation based local flexibility market for congestion management in distribution networks: Design and challenges. *International Journal of Electrical Power & Energy Systems* 156: 109742.
- Ansari MM, Guo C, Shaikh MS, et al. (2020) Planning for distribution system with grey wolf optimization method. *Journal of Electrical Engineering & Technology* 15: 1485–1499.
- Bouhouras AS, Kelepouris NS, Koltsaklis N, et al. (2024) Congestion management in coupled TSO and DSO networks. *Electric Power Systems Research* 229: 110145.
- Chakravarthi K, Bhui P, Sharma NK, et al. (2022) Real time congestion management using generation re-dispatch: modeling and controller design. *IEEE Transactions on Power Systems* 28: 2189–2203.

- Dash S and Mohanty S (2015) Multi-objective economic emission load dispatch with nonlinear fuel cost and noninferior emission level functions for IEEE-118 bus system. *2015 2nd International Conference on Electronics and Communication Systems (ICECS)*. IEEE, pp.1371–1376.
- Dehnavi E, Afsharnia S, Akmal AAS, et al. (2022) A novel congestion management method through power system partitioning. *Electric Power Systems Research* 213: 108672.
- Dehnavi E, Akmal AAS and Moeini-Aghtaie M (2024) A novel day-ahead and real-time model of transmission congestion management using uncertainties prioritizing. *Electrical Engineering* 24: 1–14.
- Derrac J, García S, Molina D, et al. (2011) A practical tutorial on the use of nonparametric statistical tests as a methodology for comparing evolutionary and swarm intelligence algorithms. *Swarm and Evolutionary Computation* 1: 3–18.
- Dolatabadi SH, Ghorbanian M, Siano P, et al. (2020) An enhanced IEEE 33 bus benchmark test system for distribution system studies. *IEEE Transactions on Power Systems* 36: 2565–2572.
- Gupta AR, Bharatbhai NM and Bhadoriya JS (2023) Performance analysis of distribution system with PV penetration using flower pollination algorithm. *Journal of the Institution of Engineers (India): Series B* 104: 441–459.
- Haq FU, Bhui P and Chakravarthi K (2022) Real time congestion management using plug in electric vehicles (PEV's): A game theoretic approach. *IEEE Access* 10: 42029–42043.
- Hobbie H, Mehlem J, Wolff C, et al. (2022) Impact of model parametrization and formulation on the explorative power of electricity network congestion management models—Insights from a grid model comparison experiment. *Renewable and Sustainable Energy Reviews* 159: 112163.
- Kamaraj N (2011) Transmission congestion management using particle swarm optimization. *J Electrical Systems* 7: 54–70.
- Liang JJ, Qu BY and Suganthan PN (2013) Problem definitions and evaluation criteria for the CEC 2014 special session and competition on single objective real-parameter numerical optimization. *Computational Intelligence Laboratory, Zhengzhou University, Zhengzhou China and Technical Report, Nanyang Technological University, Singapore* 635: 2014.
- Mahajan V, Prajapati VK and Mudagal S (2022) Review of congestion management in deregulated power system. *Deregulated Electricity Structures and Smart Grids* 32: 259–289.
- Majeed Rashid Zaidan SIT (2022) Emergency congestion management of power systems by static synchronous series compensator. *Indonesian Journal of Electrical Engineering and Computer Science* 25: 1258–1265.
- Mishra RN, Yadav A and Singh MP (2022) Artificial intelligence techniques based congestion management in restructured power systems: a review. *2022 2nd International Conference on Power Electronics & IoT Applications in Renewable Energy and its Control (PARC)*. IEEE, pp.1–7.
- Ogunwole EI and Krishnamurthy S (2022) Transmission congestion management using generator sensitivity factors for active and reactive power rescheduling using particle swarm optimization algorithm. *IEEE Access* 10: 122882–122900.
- Paul K (2022a) Modified grey wolf optimization approach for power system transmission line congestion management based on the influence of solar photovoltaic system. *International Journal of Energy and Environmental Engineering*: 1–17.
- Paul K (2022b) Multi-objective risk-based optimal power system operation with renewable energy resources and battery energy storage system: A novel hybrid modified grey wolf optimization–sine cosine algorithm approach. *Transactions of the Institute of Measurement and Control*: 01423312221079962.
- Paul K, Kumar N, Agrawal S, et al. (2019) Optimal rescheduling of real power to mitigate congestion using gravitational search algorithm. *Turkish Journal of Electrical Engineering & Computer Sciences* 27: 2213–2225.
- Paul K, Sinha P, Mobayen S, et al. (2022) A novel improved crow search algorithm to alleviate congestion in power system transmission lines. *Energy Reports* 8: 11456–11465.
- Roustaei M, Letafat A, Sheikh M, et al. (2022) A cost-effective voltage security constrained congestion management approach for transmission system operation improvement. *Electric Power Systems Research* 203: 107674.
- Saravanan C and Anbalagan P (2022) An intelligent hybrid technique for optimal generator rescheduling for congestion management in a deregulated power market. *Journal of Intelligent & Fuzzy Systems* 43: 1–15.

- Sarwar M, Siddiqui AS, Ghoneim SS, et al. (2022) Effective transmission congestion management via optimal DG capacity using hybrid swarm optimization for contemporary power system operations. *IEEE Access* 10: 71091–71106.
- Shaikh MS, Ansari MM, Jatoi MA, et al. (2020) Analysis of underground cable fault techniques using MATLAB simulation. *Sukkur IBA Journal of Computing and Mathematical Sciences* 4: 1–10.
- Shaikh MS, Hua C, Hassan M, et al. (2022a) Optimal parameter estimation of overhead transmission line considering different bundle conductors with the uncertainty of load modeling. *Optimal Control Applications and Methods* 43: 652–666.
- Shaikh MS, Hua C, Jatoi MA, et al. (2021a) Application of grey wolf optimisation algorithm in parameter calculation of overhead transmission line system. *IET Science, Measurement & Technology* 15: 218–231.
- Shaikh MS, Hua C, Jatoi MA, et al. (2021b) Parameter estimation of AC transmission line considering different bundle conductors using flux linkage technique. *IEEE Canadian Journal of Electrical and Computer Engineering* 44: 313–320.
- Shaikh MS, Hua C, Raj S, et al. (2022b) Optimal parameter estimation of 1-phase and 3-phase transmission line for various bundle conductor's using modified whale optimization algorithm. *International Journal of Electrical Power & Energy Systems* 138: 107893.
- Shaikh MS, Raj S, Babu R, et al. (2023) A hybrid moth–flame algorithm with particle swarm optimization with application in power transmission and distribution. *Decision Analytics Journal* 6: 100182.
- Shaikh MS, Raj S, Ikram M, et al. (2022c) Parameters estimation of AC transmission line by an improved moth flame optimization method. *Journal of Electrical Systems and Information Technology* 9: 25.
- Sharma P, Batish N, Khan S, et al. (2018) Power flow analysis for IEEE 30 bus distribution system. *WSEAS Transactions on Power Systems* 13: 48–59.
- Sharma V and Walde P (2022) A novel optimisation technique based on swarm intelligence for congestion management in transmission lines. *International Journal of Power and Energy Conversion* 13: 1–23.
- Sheskin DJ (2003) *Handbook of Parametric and Nonparametric Statistical Procedures*. Western Connecticut, USA: Chapman and hall/CRC.
- Srivastava J and Yadav NK (2021) Rescheduling-based congestion management by metaheuristic algorithm: Hybridizing lion and moth search models. *International Journal of Numerical Modelling: Electronic Networks, Devices and Fields* 35: jnm2952.
- Subramaniyan V and Gomathi V (2023) A soft computing-based analysis of congestion management in transmission systems. *Tehnički Vjesnik* 30: 274–281.
- Thiruvél A, Thiruppathi S, Chidambararaj N, et al. (2023) Modern power system operations in effective transmission congestion management via optimal DG capacity using firefly algorithms. *2023 9th International Conference on Electrical Energy Systems (ICEES)*. IEEE, pp.360–365.
- Verma S and Mukherjee V (2016a) Firefly algorithm for congestion management in deregulated environment. *Engineering Science and Technology, an International Journal* 19: 1254–1265.
- Verma S and Mukherjee V (2016b) Optimal real power rescheduling of generators for congestion management using a novel ant lion optimiser. *IET Generation, Transmission & Distribution* 10: 2548–2561.
- Verma S, Saha S and Mukherjee V (2018) Optimal rescheduling of real power generation for congestion management using teaching-learning-based optimization algorithm. *Journal of Electrical Systems and Information Technology* 5: 889–907.
- Wang X, Zhao T and Parisio A (2022) Frequency regulation and congestion management by virtual storage plants. *Sustainable Energy, Grids and Networks* 29: 100586.
- Wangunu IG, Murage DK and Kihato PK (2022) Power system congestion management by generator active power rescheduling using cuckoo search algorithm. *Proceedings of the Sustainable Research and Innovation Conference*, pp.159–164.
- Zakaryaseraji M and Ghasemi-Marzbali A (2022) Evaluating congestion management of power system considering the demand response program and distributed generation. *International Transactions on Electrical Energy Systems* 2022: 1–13.
- Zhou H, Lu L, Wei M, et al. (2023) Robust scheduling of a hybrid hydro/photovoltaic/pumped-storage system for multiple grids peak-shaving and congestion management. *IEEE Access* 12: 22230–22242.

Appendix

Table A1. Bid cost for the generators in the congestion management for IEEE 30-bus system (Sharma et al., 2018).

Generator number	1	2	3	4	5	6
Incremental price bids (\$/MWh)	21	19	40	42	44	39
Decremental price bids (\$/MWh)	19	18	37	36	34	38

Table A2. Bid cost for the generators in the congestion management for IEEE 118-bus system (Dash and Mohanty, 2015).

Generator number	1	4	6	8	10	12	15	18	19
Incremental price bids (\$/MWh)	39	42	40	43	21	22	44	40	43
Decremental price bids (\$/MWh)	37	34	37	38	16	17	34	37	35
Generator number	24	25	26	27	31	32	34	36	40
Incremental price bids (\$/MWh)	44	26	22	40	44	23	42	46	42
Decremental price bids (\$/MWh)	34	17	17	38	34	17	36	35	34
Generator number	42	46	49	54	55	56	59	61	62
Incremental price bids (\$/MWh)	46	44	24	31	41	42	22	25	43
Decremental price bids (\$/MWh)	37	34	17	29	35	36	16	15	35
Generator number	65	66	69	70	72	73	74	76	77
Incremental price bids (\$/MWh)	64	65	68	69	71	72	73	75	76
Decremental price bids (\$/MWh)	16	17	14	38	38	37	35	38	37
Generator number	80	85	87	89	90	91	92	99	100
Incremental price bids (\$/MWh)	79	84	86	88	89	90	91	98	99
Decremental price bids (\$/MWh)	14	37	16	35	37	37	35	36	35
Generator number	103	104	105	107	110	111	112	113	116
Incremental price bids (\$/MWh)	34	17	36	35	22	44	40	22	44
Decremental price bids (\$/MWh)	16	37	38	37	36	17	37	32	34

Table A3. Notation list.

CC	congestion cost (\$/h)	U_j	upper bounds
C_{inc}	incremental price bids (\$/h)	L_j	lower bounds
C_{dec}	decremental price bids (\$/h)	ψ	randomly generated number [0, 1]
ΔP_g	adjusted power (MW)	$Z_{m,j}^t$	mean solution
P_{Gk}	active power (MW)	$\xi_{t+1}^{(new)}$	random number [0, 1]
Q_{Gk}	reactive power (MVA)	Z_t	new position
P_{Dk}	power demand (MW)	Z_{best}	best position
θ_{kj}	admittance angle	τ	random number [0, 1]
δ_k	voltage angle	γ	Levey flight value
N_b	number of buses	RPs	reference points
N_g	number of generators	$N_{g,t+1}$	number of loads
α	convergence factor	Z	current position